Results in Engineering 11 (2021) 100257

Contents lists available at ScienceDirect

Results in Engineering

journal homepage: www.sciencedirect.com/journal/results-in-engineering

Processes and materials used for direct writing technologies: A review

Shahriar Bakrani Balani [a], Seyed Hamidreza Ghaffar [a,*], Mehdi Chougan [a], Eujin Pei [b], Erdem Şahin [c]

[a] Department of Civil and Environmental Engineering, Brunel University London, Uxbridge, UB8 3PH, United Kingdom
[b] School of Design, Brunel University London, Uxbridge, UB8 3PH, United Kingdom
[c] Department of Metallurgical and Materials Engineering, Mugla SıtkıKoçman University, Mugla, Turkey

ARTICLE INFO

Keywords:
Direct writing
Direct ink writing
Robocasting
Manufacturing
Additive manufacturing

ABSTRACT

Direct Writing (DW), also known as Robocasting, is an extrusion-based layer-by-layer manufacturing technique suitable for manufacturing complex geometries. Different types of materials such as metals, composites, ceramics, biomaterials, and shape memory alloys can be used for DW. The simplicity and cost-efficiency of DW makes it convenient for different applications, from biomedical to optics. Recent studies on DW show a tendency towards the development of new materials and applications. This represents the necessity of a deep understanding of the principles and parameters of each technique, material, and process challenge. This review highlights the principles of many DW techniques, the recent advancements in material development, applications, process parameters, and challenges in each DW process. Since the quality of the printed parts by DW highly depend on the material extrusion, the focus of this review is mainly on the ceramic extrusion process and its challenges from rheological and material development point of view. This review delivers an insight into DW processes and the challenges to overcome for development of new materials and applications. The main objective of the review is to deliver necessary information for non-specialist and interdisciplinary researchers.

1. Introduction

Additive Manufacturing (AM) is the process of automation where layers of material are deposited on top of one another to create a solid product using computer-generated models [1]. This is achievable by using appropriate materials, computer software, and a 3D printer. Compared to forming and subtractive manufacturing methods, AM technology can be argued that only the required amount of material is needed, leading to diminishing waste generation with subtractive manufacturing methods and reducing high labour intense jobs. The technology can also be argued as the industry's natural progression as it can increase safety standards, minimize construction time, and finally reduce production costs. Among several AM techniques, direct ink writing (DIW) is one of the most common methods that utilize ink-type feedstocks. This technology has been recently developed to cover all types of ceramic materials, including composites, bio-ceramics, concrete, and alkali-activated materials. DIW refers to a wide variety of extrusion-based AM processes, used for manufacturing the meso-scale and macro-scale of controlled architecture and composition parts for different applications [2]. Known as 'Robocasting' for the slurry materials and ceramics, in this process, objects are manufactured through layer by layer deposition [3]. Due to flexibility of the processes, a wide variety of appropriate materials, simplicity of the process, and creativity of the researchers all around the world, direct writing (DW) could be used for manufacturing complex functional materials and structure, and high-end products.

The fast-growing use of DW processes for different applications and materials is evidenced by recent investigations and attempts to understand and advance the knowledge in DW technology. The objectives of this review are to summarise existing technologies, process parameters, and principles adopted for DW and their applications. Latest studies on DIW and material development for different DW processes will be comprehensively presented along with current challenges with the broader applications of DW and material development.

The overall results of this review paper revealed that material extrusion is the most important and common step among all of the DW processes. Consequently, understanding the low mechanical strength, material flow, rheological behaviour and mixture optimization is necessary for most DW processes. In this paper after brief representation of the DW processes and its associate materials, ceramic extrusion

* Corresponding author.
E-mail address: seyed.ghaffar@brunel.ac.uk (S.H. Ghaffar).

https://doi.org/10.1016/j.rineng.2021.100257
Received 3 June 2021; Received in revised form 19 July 2021; Accepted 21 July 2021
Available online 27 July 2021

challenges have been review.

2. Overview of different direct ink writing processes

DW technologies mainly consist of four apparatuses, including the deposition nozzle, 3D stage, ink reservoir, and energy source. While the first three aforementioned units are common in most DW technologies, the source of energy is only used for energy-based DW processes. As shown in Fig. 1, DW is divided into three main categories: 1) extrusion-based DW, 2) continuous droplet-based DW, and 3) energy-assisted DW. These methods provide flexibility for manufacturing functional and industrial parts using different materials, complex shapes, and at various scales for different applications. In the extrusion-based DW and energy-assisted DW [4], ink is extruded through the nozzle in a continuous form, while in the continuous droplet-based DW, there is segregated droplet deposition or stream of the ink droplets, sometimes also known as Aerosol DW [5]. The solidification of the deposited ink in the energy-assisted DW is carried out by an external energy source provided to the deposition site. Contrary to energy-assisted DW, the solidification of the extrusion-based DW and continuous droplet-based DW is achieved without an external energy source. DW technologies use different types of materials, including polymers [6], metals, ceramics [7], biomaterials, human cells, piezo-electrics [8], and protein.

3. Droplet-based direct ink writing

3.1. Continuous inkjet printing system

Within the category of continuous droplet-based DW, the continuous inkjet direct writing (CIJ-DW) uses a constant flow of a binder ejected through a nozzle. After separation of the binder from the nozzle, it breaks into droplets due to a phenomenon known as Plateau–Rayleigh flow instability. Assisted by an electric field, the separated droplets are deflected to the desired location of deposition or collected to be reused [9]. The CIJ-DW methods should not be mistaken with conventional Inkjet (IJ) printing. In IJ printing, a stream of binder jets is sprayed on the power bed to solidify the powder. The two distinct principles of CIJ-DW and IJ printing are represented in Fig. 2.

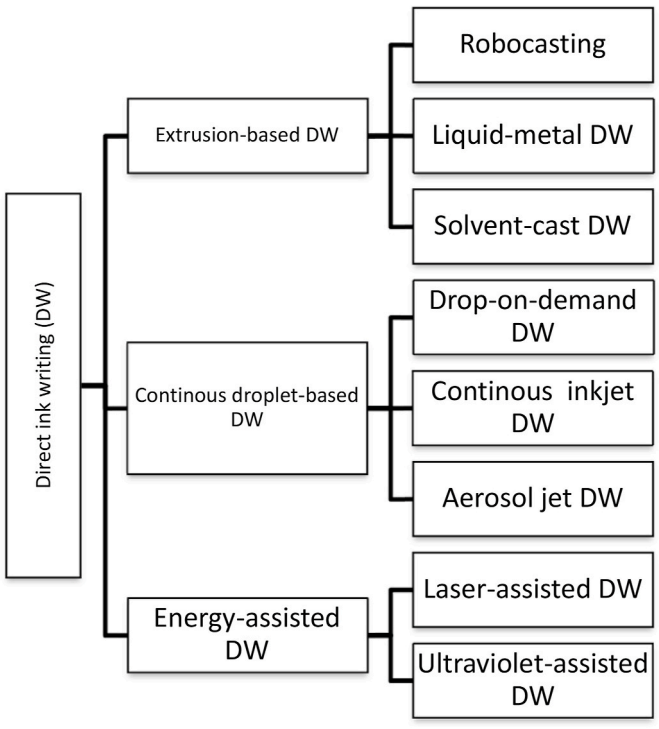

Fig. 1. Different categories and sub-categories of DW.

The important advantage of utilizing CIJ-DW is the compatibility for deposition onto different substrates such as textiles [11], Polydimethylsiloxane (PDMS) [12] and polyethylene terephthalate films [13]. Thanks to the flexibility of the process, several types of materials, including ceramic nanoparticle inks [14], metallic inks [12], polymers [15], graphene nanoparticles [16] and carbon nanotubes [17], can be used for CIJ-DW. This makes the process suitable for conductive electronic printing and textile property enhancement [11]. As shown in Table 1, the possibility of printing metallic nano-particles onto different substrates makes CIJ-DW suitable for printing electronic conduits, especially for flexible electronics. In addition, the flexibility of material selection, rapid deposition rate (200 m min^{-1}), rapid solidification of the ink, cost-effectiveness, and possibility of printing on the different types of surface are the main advantages of using CIJ-DW.

3.2. Drop-on-demand printing system

Drop-on-demand direct writing (DOD-DW) is a continuous droplet-based process, as shown in Fig. 3. In the DOD-DW process, ink is ejected from a reservoir through a nozzle to deposit the ink onto a substrate by a continuous stream of ink droplets. The continuous stream of droplets at a high frequency is created by the pressure pulse from a transducer in the extruder head. The transducers used in DOD-DW are mainly the Piezo-electric, Thermal inkjet (TIJ), and Pneumatic print heads [22]. However, several other technologies that show potential include electrospray [23], acoustic discharge [24], electrostatic membrane [25] and, thermal bimorph methods. Piezo-electric transducers are most commonly used where it works through the process of an electric field or a frequency in which the Piezo-electric materials generate sound waves within the nozzle or expand the fluid chamber to push single drops from the nozzle. One of the main disadvantages of Piezo-electric DOD-DW is that the surface tension and viscosity of the ink must be in a strict range to eject the small size of droplets. However, one of the main advantages of this technology is functionality at high temperatures up to 130 °C. To use of Thermal inkjet (TIJ) print head, the droplet is separated from the ink following the formation and explosion of vapour bubbles in the printer head. Consequently, this method is suitable for the low boiling point inks with high vapour pressure [22]. Finally, for the pneumatic print head, the actuators comprise the use of a diaphragm connected to an air reservoir. When the pneumatic pulse is applied, deformation of the diaphragm pushes a controlled amount of ink through the nozzle to perform its function [26].

A wide variety of materials could be used for DOD-DW including polymers, ceramics, biomaterials, and metals. Thanks to the flexibility of material selection, the use of DOD-DW expands from biomedical applications to electronic components. The materials used for DOD-DW in recent studies are represented in Table 2 that DOD-DW is widely used in biology and biomedical applications (see Table 3).

3.3. Aerosol jet-direct writing

Similar to DOD-DW and CIJ-DW, aerosol jet-direct writing (AS-DW) is an inkjet-based DW. In this process, ink is deposited as a spray of droplets. As represented in Fig. 4, the AS-DW method uses droplets generated by the atomizer from an active ink in the reservoir. The generated droplets are transported from the reservoir onto the deposition head by nitrogen as the carrier gas. In the deposition head, an independent nitrogen flow acting as the sheath gas is injected into the head to surround the aerosol gas. The sheath gas controls the concentration and alignment of the stream bead. There are two atomizer configurations used for AS-DW to break the ink into the fine spray of droplets [5]. In the Ultrasonic atomizer, high-frequency ultrasound capillary waves are created on the surface of the ink. The capillary waves lead to the separation of the droplets from the surface of the ink. The size of the droplets depends on the wavelength and surface tension of the ink,

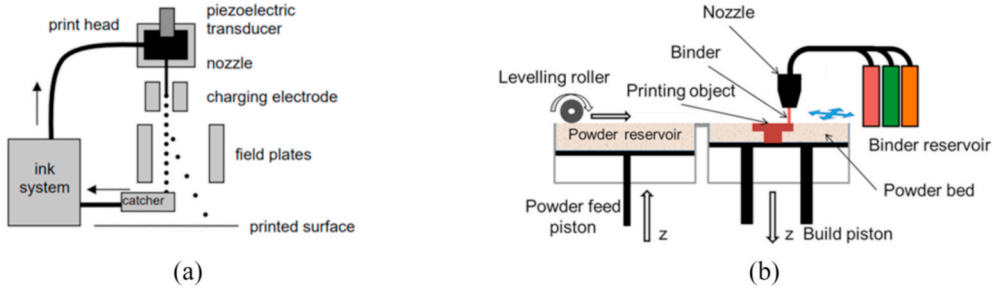

Fig. 2. Schematic representation of the (a) CIJ-DW [10] (b) IJ printing.

Table 1
Materials used for CIJ-DW and its common applications.

Applications	Materials	References
Pharmaceutical	Polyethylene glycol	[15]
	Propranolol hydrochloride	[18]
	Polyvinylpyrrolidone and thiamine hydrochloride	[13]
Textile property enchantment	Silver ink	[11]
Conductive pattern writing and flexible electronic	Conductive silver nanoparticles ink	[19]
	Carbon nanotube ink (CNT)	[20]
	Conductive silver nanoparticles ink	
	Graphene-based ink	
Energy capacitors	Multi-walled carbon nanotube (MWNT) aqueous ink	[21]
	Poly(vinylidenefluoride)- Poly(vinyl alcohol) PVDF-PVA	

Table 2
Materials used for DOD-DW and its applications.

Applications	Materials	References
Biomedical	Zirconia-based ceramic ink	[27]
	Silicone rubber	[28]
	Indium oxide (In_2O_3) and Indium tin oxide (ITO)	[29]
Biology and drug	Bovine serum albumin (Graphene additive)	[30]
	Human umbilical vein endothelial cell (HUVEC)	[31]
	Sodium alginate solution	[32]
	Green fluorescent protein D-MEM fetal bovine serum	[33]
Electronics	Nanosilver ink	[34]
Optics	PTFE (polytetrafluoroethylene)	[35]
Sensors	Ethyl cellulose (Graphene additive)	[36]
	Silicone rubber	[28]
Nano fabrications	EN 1.3505 (AISI 52100) steel	[37]
	Titanium oxide ink (TiO_2)	[29]

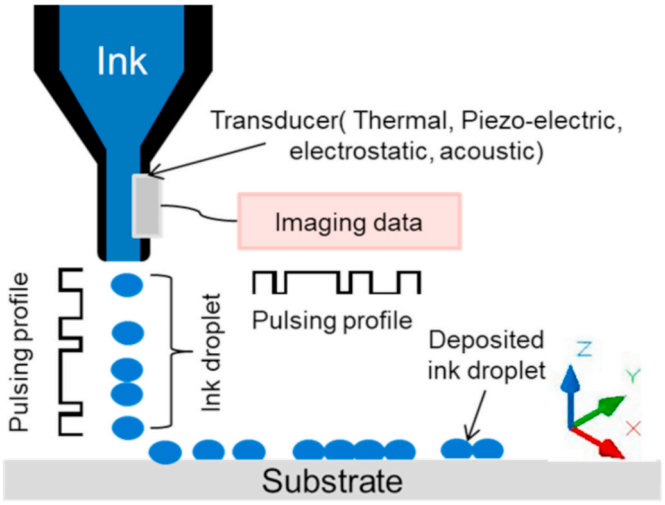

Fig. 3. Schematic representation of DOD-DW

Table 3
Application and materials used for AS-DW.

Applications	Materials	References
Biological and biomedical	Clariant® silver ink, Gelatin Poly-L-lysine	[41]
	Acrylates and methacrylates, Polydimethylsiloxane (PDMS)	
Aerospace and communication	Silver nanoparticle ink	[42]
Biosensors and sensors	graphene: Nitrocellulose powder, poly(3,4-ethylenedioxythiophene) polystyrene sulfonate (PEDOT:PSS)	[43]
Micro manufacturing and microfluid	Polydimethylsiloxane (PDMS)	[44]
Optics	Polydimethylsiloxane (PDMS)	[45]
Transistors	commercial ink (IsoSol-S100) with carbon nanotubes	[46]
	Ink with carbon nanotubes	
Battery and energy storage devices	PEO (Polyethylene oxide)	[47]

while the required power to atomize the ink highly depends on the viscosity of the ink [38]. For pneumatic atomizers, also known as "two-fluid atomisation", is a process in which high-velocity gas causes a disruptive action that produces sprays in a stream of liquid. Several applications, including mass-transfer operations, coating of surfaces and particles and fuel atomisation in combustion processes, have been reported to atomize liquids into multiple droplets [39].

AS-DW is a promising technology for the fabrication of interconnects, sensors and thin-film transistors. The main advantage of AS-DW methods is the possibility of depositing on different types of substrate.

The parameters of the AS-DW process are generally divided into several categories, including ink properties, process, print head and deposition parameters. One of the drawbacks of AS-DW is its high dependency on the particle size, viscosity and saturation ratio of the ink in the reservoir. At higher concentrations, bigger particles separate from the surface of the ink in the reservoir, while finer particles separate from the ink surface. This leads to variation in the dimensions of the deposited inkjet beads that may cause issues at lower concentrations.

4. Energy-based direct ink writing

4.1. Laser-assisted direct ink writing

As described in Fig. 5, laser-assisted direct writing (Laser-DW) brings together the ink extruder and a focused laser beam to produce complex shapes. Similar to extrusion-based DW material, the ink is extruded from the nozzle in a desired pattern onto a substrate. Upon exiting the material from the nozzle, the deposited pattern is rapidly heated to solidify, thereby reaching a certain mechanical strength. Generally, the materials

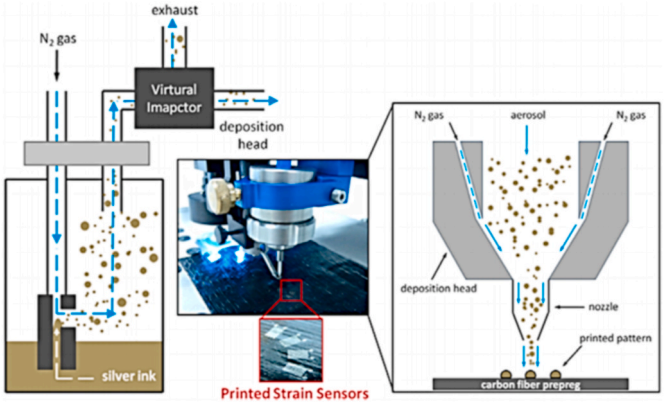

Fig. 4. Representation of the principe of AS-DW [40].

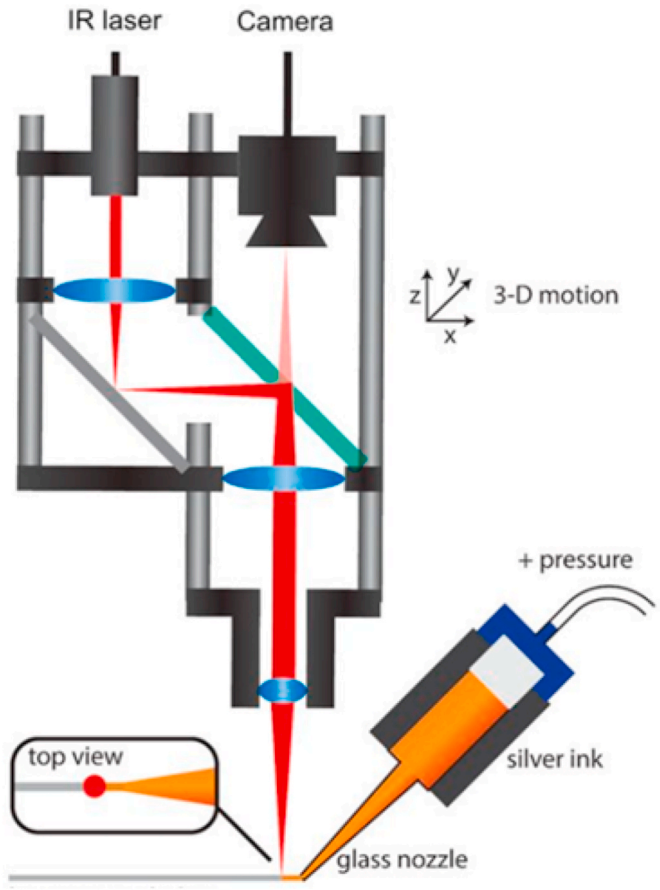

Fig. 5. Schematic representation of the Laser-DW [60].

suitable for Laser-DW consists of at least two key components [48]. Firstly, it requires a Photoinitiator that absorbs the laser light that provides the activation for polymerisation. Examples of photo-polymerisation agents include acrylic photopolymer [49], SU-8 epoxy-based photo-resist [50], hybrid silicate-only based photopolymers [51], Hydrogels such as polyethylene glycol [52], and natural polymers like crosslinked proteins such as fibrinogen, fibronectin and collagen [53]; and chemically modified natural polymers such as photo-structural composites based on polycaprolactone [54]. The second component for Laser-DW is a monomer or a mixture of monomers/oligomers that provide the final polymer. Almost all types of materials could be used for Laser-DW including polymers [55], metallic composites [56], biomaterials, graphene composites [55], carbon nanotubes pastes [57], etc. Due to the flexibility of Laser-DW on material selection, it covers a wide range of applications such as biomedical, optics, electronics and shape-memory materials (Table 4). Recent publications on Laser-DW show a growing interest in developing the new inks [58] and broader industrial applications [59].

4.2. *Ultraviolet-assisted direct ink writing*

Ultraviolet-assisted direct writing (UV-DW) is an extrusion-based technology that uses ultraviolet light to initiate a photochemical reaction that leads to crosslinks of the molecular chains of the resin or the thermoplastic material, as depicted in Fig. 6. For certain materials, the printed part is placed inside an oven to achieve its final strength.

Because of its characteristics including low-temperature processes, high mechanical performance and low-energy requirements, UV-DW is widely used to produce coatings, electronics, robotics, optics, etc. The potential applications and materials used for UV-DW are shown in Table 5. One of the main advantages of UV-DW is the speed of the process. Because of the fast setting time of the ink, its solidification takes place fast after the deposition. This avoids the spread of the wet ink due to the flowability of the substance; consequently, by using UV-DW, the printed parts have more consistency in terms of their shape and geometry.

In addition to normal extrusion-based DW parameters, it is necessary to also control the intensity of the UV light to achieve consistency in the production.

5. Extrusion-based direct ink writing

5.1. *Liquid metal direct writing*

Liquid metal direct writing (LM-DW) is the common AM process for low viscosity, low melting temperature metals, and other conductive materials [67]. As shown in Fig. 7, the metal liquid is extruded through the nozzle and deposited onto a substrate. Table 6 represents the applications and materials used for LM-DW and the substrate. According to the aforementioned properties, only Mercury (Hg) and Gallium (Ga) are suitable for the LM-DM process. However, because of the toxicity of Hg, it is no longer used. The inherent properties of Ga-based alloys, such as low toxicity, low viscosity and low melting temperature, make it the most widely-used material for LM-DW (Table 4). Since LM-DW is suitable for manufacturing conductive materials, it is widely used to manufacture electronic and stretchable conductive materials [68]. Recent research on LM-DW is mostly focused on the adhesion between the ink and the substrate [69]. The new ink development for the LM-DW is limited to adding Nano Carbon Tubes (CNT) [70], Cu nanoparticles [71] and Gallium composites. Similar to extrusion-based DW technologies without energy-assisted methods, the process parameters are the nozzle, the ink composition and additives, nozzle geometry and the printing pattern (see Fig. 8).

5.2. *Solvent-cast direct-write*

The principles of solvent-cast direct writing (SC-DW) are relatively

Table 4
Application and materials used for Laser-DW.

Applications	Materials	References
Shape memory materials and functionally gradient materials	Carbon paste, silver paste, nickel paste, and nano-particle silver inks	[57]
	Supramolecular cholesteric liquid crystalline	[58]
Optics	Polydimethylsiloxane (PDMS)	[55]
Electronics	Copper/Graphene-based ink	[59]
Biology	Polydimethylsiloxane (PDMS)	[61]
Wearable electronics	Graphene-based ink	[62]

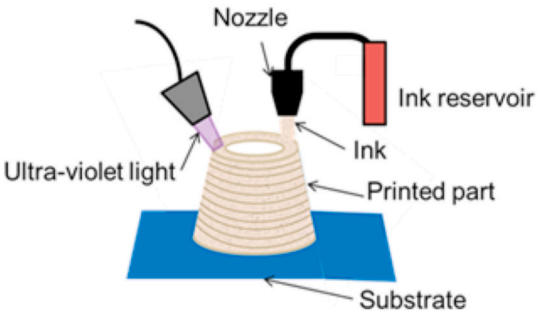

Fig. 6. Schematic representation of the ultra-violet assisted direct writing.

Table 5
Application and materials used for UV-DW.

Applications	Materials	References
Nanocomposites	Carboxylated styrene-butadiene rubber (SBR) latex (silica nanoparticles)	[63]
Automobile industry to aerospace.	Bismaleimide	[64]
	Isocyanate ester thermosets	[65]
Actuators, robotics	Acrylate-based amorphous polymers (fumed silica nanoparticles and NdFeB microparticles)	[66]

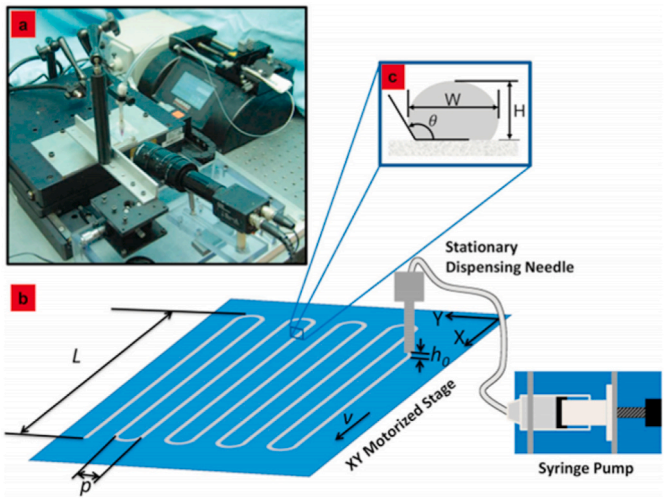

Fig. 7. Liquid metal direct writing system. a) Photograph of a LM-DW apparatus. b) Schematic or LM-DW pattern. c) Detail of the cross-section of the deposited bead by LM-DW [72].

similar to extrusion-based direct writing. In this process, thermoplastic solution ink is mixed with a rapid evaporable solvent extruded through the nozzle. Rapid evaporation of the solvent further leads to rapid solidification of the ink. This phenomenon makes SC-DW suitable for printing without support structures that makes this process suitable for manufacturing shape-memory materials, biomedical parts and for tissue engineering.

Because of the importance of ink rheology, recent publications on SC-DW have focused on ink composition and preparation [79] and the development of new solvents [80]. Furthermore, the simplicity of the process makes it applicable for nanoparticle composites such as carbon nanotubes [81], Silver micro flakes [82], and Magnesium nanoparticles [79]. The possibility of adding nanoparticles also enables the manufacturing of conductive materials [83]. The potential applications and a summary of the solvents and additives used for SC-DW is shown in Table 7. Dichloromethane (DCM) are the most commonly used solvent ink in the SC-DW process. Several studies have been carried out to examine the influence of different solvents on printed parts [84]. It should be mentioned that the polymers are mostly utilised as a binder for SC-DW. A summary of solvents and binders for SC-DW is presented in Table 7.

Table 6
Application and materials used for LM-DW.

Applications	Materials	Substrate	References
Flexible and stretchable electronics	The eutectic alloy of Gallium, indium, and tin (Galinstan) EGaIn	silicone elastomer (polydimethylsiloxane (PDMS))	[68]
	EGaIn	Printing paper, Polystyrene, Kaprone tape, Polyethylene, Scotch tape, Weight paper, Silicone, Aluminium foil, Glass slide, Si wafer, gold-coated Si wafer, Si wafer with an oxide layer, Copper foil, Sapphire, Wood, Steel plate	[69]
		Glass, Si wafer, PVMS, Sylgard©-184, SEBS, Dragonskin©, EcoFlex©, Teflon	[73]
	EGaIn	PDMS Ecoflex	[74]
		ENIG, Im-Ag, E-less Ni, OSP, Im-Sn, Dragonskin	[75]
	Galinstan (additives: Cu, Ni, and Ag nanoflakes)	Styrene–isoprene styrene	[71]
Strain sensors	GaIN	TPR elastomer	[76]
Terahertz Technologies	EGaIn liquid alloy	DOW CORING Glass Silicone Sealant	[77]

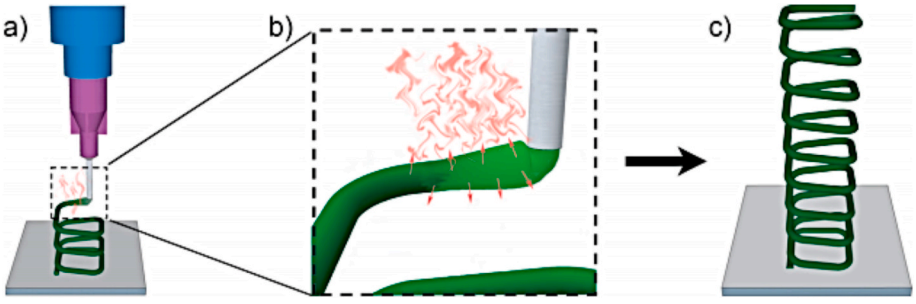

Fig. 8. Schematic representation of the solvent-cast direct-write. a) Deposition of the solvent through a nozzle. b) Evaporation of the solvent after the extrusion. c) Final product manufactured by SC-DW [78].

Table 7
Some of the materials used for the SC-DW.

Application	Binder	Solvent	Additive	References
Bone and tissue engineering	Polystyrene	Chloroform	Mg powder	[79]
	Polycaprolactone (PCL)	chloroform (CF) Dichloromethane (DCM) Toluene (TOL) acetic acid (AA) Acetone(ACE) dimethylformamide (DMF) Dimethyl sulfoxide (DMSO)		[80]
	Matrimid 5218	Tetrahydrofuran (THF)		[23]
	PLLA	DCM Dibutyl phthalate (DBP)	Raw α-chitin	[85]
Electronic and electric	Polymethyl methacrylate (PMMA)	Anisole	Silver micro flakes	[82]
	PLA	Dichloromethane (DCM)	Ag-coated CNFs	[83]
Shape memory	Poly(D,L-lactide-co-trimethylene carbonate) (PLMC)	DCM	Carbon nanotubes (CNTs)	[86]
	PLA	DCM Polyesteramide	Carbon fiber Barium titanate	[81]
Biomedical and prosthesis	Polycaprolactone (PCL)	DCM and Acetone (ACE)		[87]
	PCL(polycaprolactone)		Peptide	[88]
	poly(lactic-co-glycolic) acid (PLGA) Polystyrene(PS) Polyethylene oxide (PEO)	DCM		[89]
	Polycaprolactone	DCM and methanol Dicyclohexylcarbodiimide (DCC) Dimethylaminopyridine (DMAP) Dimethylformamide (DMF) Camphorsulfonic acid (CSA)		[84]
Manufacture of Isotropic Thin Films	PLA	Chloroform Dimethylacetamide (DMAc) Polyvinyl alcohol (PVA) Polybenzimidazole (PBI)		[90]

5.3. Robocasting

The extrusion-based direct writing or robocasting is the most common and simplest process among all the DW processes. In this process, material flows through a nozzle and is deposited on a 3D stage according to a predefined generated path translated to the codes. Close to the material extrusion process, robocasting is mainly used for liquids [91], hydrogels [92], colloidal gels [93], suspensions pastes, and cementitious inks. Unlike fused filament fabrication (FFF), material deposition occurs at room temperature in the robocasting process. Consequently, unlike the FFF process and other additive manufacturing with high processing temperature, manufactured parts by robocasting do not suffer from thermal and residual stress [94]. On the other hand, due to the shear-thinning behaviour, the extrudate ceramic pastes experience a rapid increase of viscosity after deposition upon drying [95]. The nozzle diameter of the ceramic extruders are typically in the range of 100–1000 μm and can produce relatively simple architectures due to their inability to self-support. Nevertheless, high-density robust constructs can be obtained by conventional sintering after robocasting due to its ability to uniformly pack particles under high deposition pressures [96].

The solidification of the ink in DW depends on the setting time of the ink. Consequently, optimization of the ink properties, including setting time and rheological properties, are crucial for the direct writing process. The optimization of the setting time and rheological properties could be done by adding additives during ink preparation and selecting the best printing parameters and printer structure. Several categorise of additives, including reinforcing agents, rheology modifiers, thixotropy modifier, retardant and, dispersant have been employed to optimize the printable inks. However, the composition and ratio of each additive must be accurately controlled to satisfy the desire properties (i.e. enhanced mechanical properties, shape stability, bio-computability, size, etc.) of the final part. In the following sections, different additives used for cementitious composites in robocasting are discussed. In addition to modifying the paste composition, printer structure should be selected according to the paste rheological behaviour. While the motion mechanism is similar in all printers, the pressure mechanism varies according to rheological properties of the paste. Two mechanisms have been utilised to pressurise the ink in robocasting: 1) applying the normal stress by a plunger in the barrel or 2) applying the shear stress by a screw mechanism. The latter is more effective in ink transport due to the higher contact surface area. However, more complex to design compared to the simple plunger. The plunger mechanism could be used for the paste with higher flowability (lower viscosity), while the screw mechanism is effective for complex pastes with low flowability. The plunger mechanism and screw extruder mechanism are illustrated in Fig. 9.

The selection of printing parameters highly depends on the material's rheological properties, ink composition, and printer structure. For high-viscosity pastes, the printing pressure is higher than low-viscosity pastes. Furthermore, printing the same paste with a small diameter nozzle requires more pressure than printing with a bigger nozzle. However, the dimension selection of the nozzle depends on the size and precision of the desired part. The printing parameter for DW includes nozzle diameter, printing pressure, ink flow rate, the height of the layer,

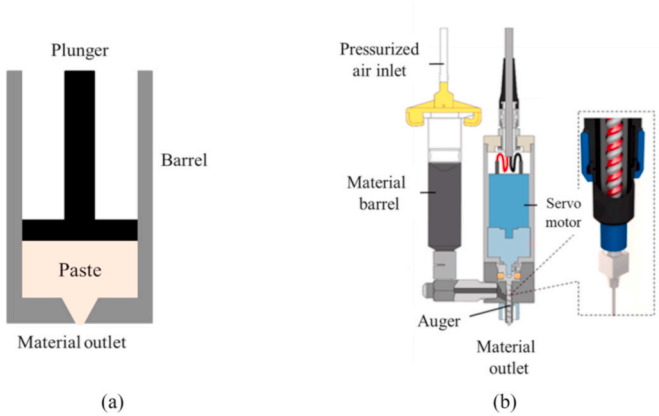

Fig. 9. Two mechanisms used for the DW (a) Plunger mechanism, (b) Screw extruder mechanism [97].

layer thickness, filling pattern, printing speed, filling density, paste open time, paste setting time, etc. Besides the paste composition optimization, the printing parameters must be selected delicately. Table 8 represents the printing parameter range for DW of CaP paste. As it is pointed in Table 8 the printing parameters compromise a relatively wide range (i.e. printing pressure 0.5–6 bar). This is mainly because of the ink composition and additives (see Table 9).

5.3.1. An overview of materials flow mechanisms in extrusion-based DIW

Ink deposition in DW systems is commonly facilitated by constant displacement of the plunger so that ink filaments are extruded at a uniform volumetric flow rate. The filament diameter is determined by the nozzle diameter, ink rheology, and flow rate. The ink flows through the deposition nozzle when a pressure gradient is applied along the nozzle length. The resulting shear stress on the suspension is represented as (Eq. (1)):

$$\tau_r = \frac{\Delta P^* r}{2l} \quad \text{Eq. 1}$$

where r is the radial position within the nozzle, ΔP is the pressure drop and l is the nozzle length. Shear stress at the wall of the nozzle is related to the shear rate, $\dot{\gamma}$ for a Herchel-Bulkley type fluid according to Newton's law of viscosity (Eq. (2)):

$$\tau_R = \tau_Y + m\,\dot{\gamma}^n \quad \text{Eq. 2}$$

where is the yield strength, m is the consistency index of viscosity for Newtonian fluids, and n is the shear rate dependency index.

A velocity profile is obtained by integration of Eq. (2) between the two boundary points of $r = 0$ and $r = R$ in a cylindrical nozzle. As schematically represented in Fig. 10, the velocity profile generally consists of a plug and laminar flow regions for stably flowing suspensions. Plug flow is characteristic of suspensions exhibiting some degree of plasticity and the consequent yield strength. The core of the suspension always flows as an unyielding plug with constant velocity. This volume is surrounded by a transition zone of laminar flow with the varying velocity that ends at the wall at a thin apparent slip layer of thickness δ that consists solely of the liquid phase of the suspension. This is because, during the flow of a suspension of rigid particles, the particles cannot physically occupy the space adjacent to a wall as efficiently as they can far away from the wall.

For concentrated suspensions of rigid, low-aspect-ratio particles, slip-layer thickness δ scales with the particle diameter D_P. Various investigations have determined the values of the ratio δ / D_P in the range of 0.04–0.07 [106]. For solid loadings less than the maximum packing fraction ($\varphi < \varphi_{max}$), the slip-layer thickness is a function of the solid loading, average size, and maximum packing fraction as [107].

$$\frac{\delta}{D_P} = 1 - \frac{\varphi}{\varphi_{max}} \quad \text{Eq. 3}$$

For the screw-driven pressurization mechanism, the flow regime is relatively simple. Here the rotation rate of the screw is the control parameter and a line on the screw surface can be schematically represented in two dimensions by the plane Couette geometry shown in Fig. 11. The screw acts as a spirally moving plate to drag the fluid forward due to its forward inclination towards the barrel wall, which acts as the stationary plate. Compared to plunger-induced flow, this method has the advantage of the lack of a pressure build-up at the material as the stress is transferred mainly by the screw, not the material. As a result, there is no partial plug formation moving at the maximum velocity away from the walls.

Table 8
The range of printing parameters for ceramic robocasting.

Parameter	Range	References
Printing pressure (bar)	0.5–6	[98–100]
Nozzle diameter (mm)	0.1–0.85	[100–102]
Printing speed (mm.s^{-1})	2.5–20	[96,100]
Layer thickness (mm)	0.075–0.4	[99,101,103]
Filling gaps (mm)	0.2–1.2	[98,104]

Table 9
Summary of the materials used for the robocasting.

Application	Material	Additive	References
Bone and tissue engineering	Hardystonite (Ca_2ZnSi_2O7)	–	[119]
	Hydroxyapatite	–	[120]
	Hydroxyapatite	Plasticizer PEG	[121]
	HA/β-TCP	Plasticizer PVB/PEG	[122]
	Zirconia-toughened alumina (ZTA)	–	[123]
	Polycaprolactone (PCL)/hydroxyapatite (HA) and PCL	–	[124]
	β-Tricalcium phosphate	–	[110,125,126]
	Bioglass 45S5 or calcium sodium phosphosilicate	SiO_2 or B_2O_3	[104]
	Bioactive 6P53B glass	–	[101]
	alpha-TCP cement	Plasticizer gelatin	[125]
	Bioactive 13–93B3 glass	Plasticizer ethyl cellulose	[113]
	CaP glass	Plasticizer PLA/PEG	[127]
	Titania	Plasticizer Na-alginate	[74]
	Zirconia	Plasticizer PVA	[128]
	Alumina	Plasticizer Aquazol, PEG	[16]
wave-transparent ceramics	Phosphate inks	Rheology Modifier and reinforced agent: SiO_2	[129]
Optic	Yttrium aluminium garnet (YAG, $Y_3Al_5O_{12}$)	–	[130]
Electronic, electric, and insulation	Si2N2O	–	[131]
	SiC	Short carbon fiber	[132]
	Kaolin clay ($Al_2Si_2O_4$)	–	[133]
	CABS/ZnO	–	[134]
	NiZn-ferrite	–	[135]
	Lead-zirconate-titanate	Plasticizer cellulose	[115]
	Silver	Ethylene glycol	[136]
	BaTiO3	Gelation agent ammonium chloride zinc acetate, Plasticizer PVA	[137]
Manufacture of interpenetration phase composites	Al2O3 and ZrO2, with Al infiltration	Gelation agent polyethyleneimine	[138]
Water and waste water treatment, catalyst support, filtration membranes	Chamotte (CH) and alumina-zirconia-silica (AZS)	Alkaline solution	[139]
	Alumina	Plasticizer Polyvinylpyroline	[140]
Refractory	Alumina	Silica fume	[16]
	Spinel	Gelation agent methyl cellulose	[140]
Flame retardant additive for fire-safe polymers.	Boehmite		[141]
Lightweight composite gears	Alumina powders and platelets	Plasticizer pluronic copolymer	[96]
Nanocomposites for energy applications	Graphene oxide	Branched copolymer surfactant	[137]

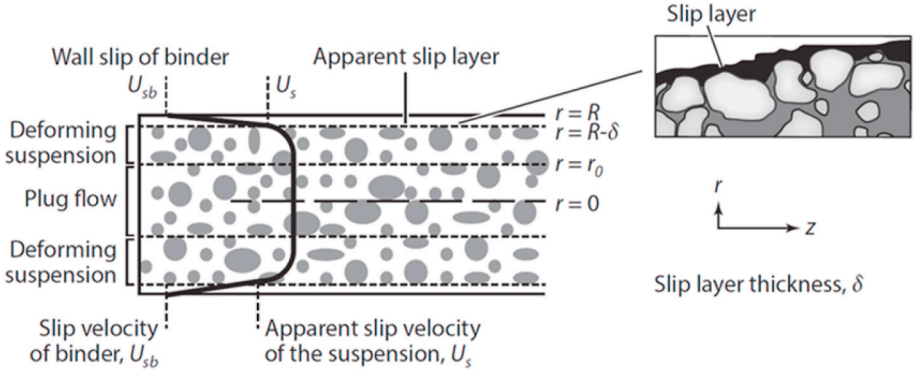

Fig. 10. The velocity profile of a concentrated suspension undergoing apparent slip at the wall of a cylindrical tube [105].

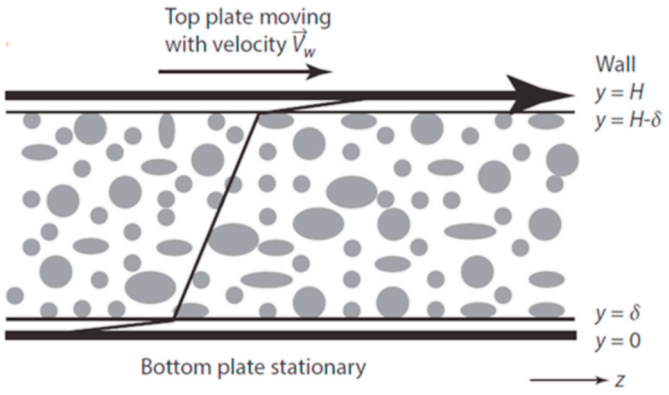

Fig. 11. The velocity profile of a concentrated suspension undergoing apparent slip at the wall of a sliding surface (plane Couette) [105].

The analysis of wall-slip is especially important for DIW micro-extrusion and injection applications because it presents the loading conditions required for a stable flow of suspended particles through narrow capillaries. Accordingly, the shear stress at the capillary wall should exceed a threshold value to cease complete plug flow and initiate partial plug flow with a deforming region. Further refinement of the theory by Tang and Kalyon defined the contiguous slip condition that occurs at a shear stress level well above this critical shear stress as the remedy to the phase separation and the associated flow instability and clogging problems [108]. It has been empirically validated by studies on the injection issues for inorganic bone cements and suspensions [109] and by robocasting studies as well [110].

5.3.2. Materials for extrusion-based DW

Due to the simplicity of the robocasting process, many studies have been conducted to broadening applicable materials for robocasting and its applications. A wide range of ceramic-based materials, polymers with low melting temperature and thermosets, clay-based materials, and metallic additives are successfully printed by robocasting such as silk [111], graphene [100], lead zirconate titanate [112], bio-glass [113]. Filaments are commonly deposited and dried in humidified air or another slow-drying medium such as oil because of the common risk of clogging due to fine nozzles, fast-drying rates and the need to have asmall binder in ink. In addition to simple drying, the viscoelastic transition of inks is facilitated by other sophisticated methods like physically gelling polymeric binders [114], reversible electrostatic destabilizing sols [115], thermally reversible hydrogel binders [96], pH-reversible hydrogel binder [100], and spider-web imitation poly-electrolytes [95].

Inorganic powder suspensions generally may make up problematic inks for robocasting compared to polymer suspensions due to their tendency for sedimentation and separation from the binder. They are mostly utilised as inks in sizes close to the colloidal range for electrostatic stabilization and with the help of processing aids that promote their dispersion and adhesion with the suspending medium.

Inks made of non-setting, concentrated ceramic suspensions should be conditioned to exhibit indefinite stable flow behaviour as a prerequisite of a reliable DIW assembly capable of working for many hours without clogging. Robocasting inks must generally fulfil three requirements:

1. They must exhibit a well-controlled viscoelastic response such that they set once deposited to facilitate shape retention of the structure and fusion with the previously deposited material;
2. They must contain a high solid volume fraction to minimize drying-induced shrinkage so that the particle network is able to resist compressive stresses arising from capillary tension;
3. They must have a homogeneous particle distribution to ensure flow stability;

The electrostatic forces between the particles and the binder need to be controlled carefully to meet these criteria by first stabilizing a highly filled suspension and then inducing a phase change to cause a viscous-to-elastic transition in flow behaviour. This strategy has been used to produce colloidal inks from various ceramic materials [116]. Another common strategy to optimize ink rheology has been the calcination of the particles prior to ink preparation. Although this is expected to affect the adhesion between the solid and liquid phases adversely, it reduces the effective solid loading and does not significantly alter the particle size. Hoelzle et al. investigated the effect of calcination time for hydroxyapatite particle-containing inks. They reported that the viscosity decreased from 236 Pa s to 66 Pa s while the shear thinning index stayed constant at 0.35 by increasing the calcination time at 1100 °C from 30 min To 10 h (both proceeded by 13 h ball milling in ethanol) [117]. This strategy is a trade-off between ink extrudability and filament rigidity that may backfire in the case of large particles due to insufficient grinding, resulting in significant phase separation and variations in filament density [118].

In addition to the aforementioned criteria for ink preparation (ink composition and additives, particle size), the printing parameters and printer structure must be precisely selected for each material. Compatibility of the additives and reinforcement agents with binder and potential applications are the main criteria to be considered during ink development. The ink development must be with regard to the printer structure, printing parameters such as nozzle diameter, and the size of the final desire product.

In this review paper among the aforementioned materials for extrusion-based DW, the 3D printing challenges for ceramics and cementitious-based materials have been reviewed. The challenges for 3D printing of ceramics and Cementitious composites, including

Injectability, rheology properties, bridge fabrication without support, shape retention and, nozzle clogging, have been discussed in the following sections.

5.3.3. Challenges in ceramic composites direct writing

5.3.3.1. Injectability. One of the main drawbacks of cementitious DW is phase separation. Phase separation refers to the separation of the powder substance from the liquid during material extrusion through the nozzle attributed to faster travel of the liquid phase than powder during extrusion, which leads to variation between the ratio of the solid phase to liquid phase [142]. The higher liquid content after deposition leads to a reduction of the viscosity, an increase of setting time, reduction of the paste adhesion, and therefore a decrease in the mechanical properties of printed objects. Furthermore, a higher ratio of powder remains in the barrel of extruder, which leads to nozzle clogging and blockage [143]. The phase separation in extruders could be quantified by the injectability notion [142]. The injectability is known as one of the most critical properties of cementitious composites printing and is defined as the extrudate mass to the mass of the initial paste [144]. Many studies have been conducted to improve the injectability of the ink for robocasting [145]. Several methods have been reported to improve the injectability of cementitious composites. It is necessary to (i) reduce the extrusion pressure, which could be done by increasing the flowability, decreasing the viscosity or the shear thinning index of the ink or extruding through a larger/shorter channel and (ii) increasing the pressure required to force the liquid flow through the powder particles (P_{ps}). P_{ps} could be determined for Newtonian fluids using Eq. (4) [143].

$$P_{ps} = \frac{Q\eta_0 l}{kA} \quad \text{Eq. 4}$$

where Q is the volumetric flow rate, η_0 is the viscosity of the liquid, l is the length of the powder bed, k is permeability and A is the cross-sectional area of the powder bed. The well-known Krieger-Dougherty equation (Eq. (5)) for concentrated suspensions also applies to DW inks:

$$\eta_S = \eta_0 * \left(1 - \frac{\varphi}{\varphi_{\max}}\right)^{-B\varphi_{\max}} \quad \text{Eq. 5}$$

where η_S is the suspension viscosity that changes as a function of the liquid viscosity η_0, the solid volume fraction φ, the maximum packing fraction $\varphi_{\max}$, and the intrinsic viscosity B which is generally taken as 2.5 for rigid spherical particles in the suspension. An alternative form of this equation can be written in terms of the slip layer thickness and the mean particle size in place of the paranthesis. Many rheological studies on ceramic suspension have given empirical validation of this equation. For instance, in case of Calcium Phosphate (CaP) printing, the following procedures can be employed to improve the injectability:

- The viscosity of the liquid phase: it has been observed that increasing the viscosity of the binder or the interface area around the particles by size reduction lead to higher P_{ps} and consequently, improvement or elimination of the phase separation. Bohner et al. revealed that incorporation of xanthan as an additive improves the injectability of the CaP [144]. Franco et al. decreased the printing pressure by adding Pluronic_ F-127 solutions to the CaP paste. Their experiments revealed that by improving the injectability, the material could be printed by a nozzle as narrow as 0.1 mm in diameter [110]. Other studies show that the inclusion of additives such as cellulose ethers [146], gelling agent [147], and glass beads (Spheriglass) [148] lead to improved injectability of the CaP. The most direct way to increase the viscosity of the liquid phase is to cool it. This approach is commonly followed by the Freeze-Form Extrusion variant of the robocasting process. The ink is processed at lower temperatures than the ambient temperature, with better flow stability and frozen upon deposition on a stage kept at sub-zero temperatures [149].
- Maximum packing fraction: in addition to enhancement of liquid phase viscosity of the cementitious paste, it is necessary to optimize the solid phase of the paste. Both powder particle and packing solid volume fraction play an important role in the permeability and injectability of the paste. The paste's liquid phase should fill voids between the powder particles. The presence of excess liquid, increases the distance between particles and, consequently, the flowability of the paste. Increasing the flowability of the paste by increasing the liquid to powder ratio (LPR) results in an improvement in injectability [150]. Flowability could similarly be improved by modification of particle size [151], particle size distribution [152] and, particle shape [153], which directly affect the intrinsic viscosity and the maximum packing fraction.
- Particles interaction: the strength of the particle network highly depends on the interaction between paste's particles. It has been shown that friction reduction between the particles leads to increased flowability and consequently injectability [154].
- Setting time: it has been observed that the inclusion of a setting agent to the mixture leads to an increase in friction between the particles. An increase in the friction between particles causes a decrease in the injectability of paste [125,154,155].
- Extrusion parameters: other parameters influence the injectability of the ink, such as nozzle dimension [142,149] and the uniformity of the paste mixture [156].

5.3.3.2. Fresh properties. Fresh properties (i.e. dough time, initial setting time, final setting time, and open time) are primary rheological properties of the paste to be considered for robocasting. As pointed in Fig. 12, the initial setting time is defined as the time paste starts to harden after mixing. The final setting time refers when curing of the paste is completed and the flowability of the ink is tends to zero (i.e. paste complete solidification). Close to the initial setting time, paste has high flowability and low viscosity and close to the final setting time the viscosity of ink drastically increases and flowability decreases as evidenced by the exponential nature of their pressure vs. time/displacement curves [157]. Although initial and final setting times are important for DW of cementitious composites, they could not provide the printing window of the inks. Therefore, the printing open time is defined as the printable time of the paste. For a suitable printable paste, the open time must be long enough to cover the period of adding paste into the reservoir barrel of the printer until material deposition. Short open time means the fast setting of the paste in the reservoir and extruder. Consequently, it is necessary to improve the rheological properties to elongate the open time of the ink [158]. This could be done by adding rheology modifier agents [29], retardant materials, or applying pre-shearing to the ink [159]. The rheology study of the ink is a key point for the development of new inks for DW. The fresh properties

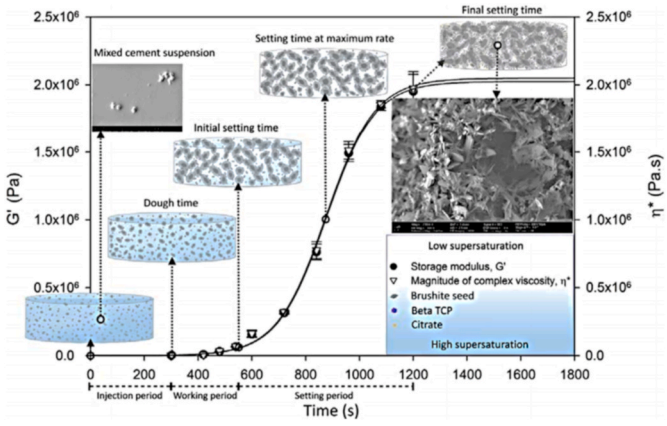

Fig. 12. Illustration of the fresh properties for CaP [159].

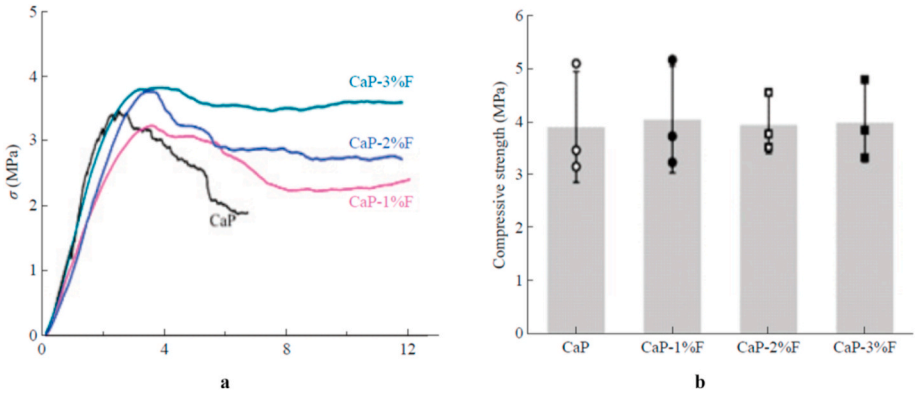

Fig. 13. Mechanical strength of the robocasting part in CaP (a) stress-strain (b) compressive strength [182].

could be determined by measuring the rheological properties such as yield shear stress, apparent viscosity, plastic viscosity, loss (G") and storage (G') modulus and complex viscosity (η*) [160] (see Fig. 13).

The rheological properties are also predominant parameters on the shape stability and quality of interlayer bonding of the deposited filaments in robocasting. Low viscosity leads to poor shape stability and collapse of deposited materials. On the other hand, high viscosity results in poor interlayer bonding and cohesiveness [161]. Several criteria have been suggested in order to improve printability and to control the deposited material's slump. For instance, Li et al. suggest that for the polymer DW the difference between the storage modulus (G′) and loss modulus (G″) should be lower than 0.8:1 [162]. Different studies revealed the necessity of high storage modulus and yield stress for DW of ceramic pastes. Zocca et al. indicated that for the ceramic pastes, storage modulus should be in the range of 105–106 Pa and yield stress in the range 102–103Pa [145]. Other authors suggested that the storage modulus must be more than 2000 kPa and the yield stress must be more than 200 Pa [163]. Shareen et al. proposed that buckling and yield stress is the key properties for structural stability. They introduced an equation (Eq. (6)) relating G′ and τ_y , which forms the boundary transitioning from good printability to slumping [160].

$$G' = \frac{K}{\tau_y} \qquad \text{eq. 6}$$

where K is a constant. They have suggested that sufficiently high product of the yield stress and the storage modulus is necessary in order to avoid the slumping [160].

The cement robocasting technique may be further refined to utilize fast-setting cements by careful *in situ* control of the setting kinetics. This has not been possible by conventional methods employing plungers to induce pressure. Understanding of pre-shearing as a means to physically alter the evolution of dynamic cement microstructure and control the cement setting kinetics has opened the way to improvements in cement handling and processing [164]. This novel physical treatment of cements was developed based on the observations that subjecting a cementitious calcium phosphate suspension to torsional strains in various shearing modes and according to cement-specific critical shearing conditions can significantly increase or decrease the setting time and the resultant viscosity [159]. It provides control on the thixotropy of cements by inducing favourable mechanical responses to imposed shear strains for contiguous wall slip and stable flow.

5.3.3.3. Fabrication of the bridge without support by 3D printing. Another drawback of the extrusion-based DW is the lack of shape retention during bridge deposition without the supports. Depending on the rheological properties, shape retention of the deposited bridge is crucial for the form stability of the part. Smay et al. considered the deposited filaments as beams with circular cross-sections supported at both ends and calculated the deflection Δ as a function of the physical properties of the ink and the filament using Eq. (7) [115].

$$\Delta = \frac{2(\rho_{ink} - \rho_{med})gy\left(2Ly^2 - y^3 - L^3\right)}{3ED^2} \qquad \text{Eq. 7}$$

where ρ_{ink} is the density of the ink, ρ_{med} is the density of the deposition medium (commonly air or oil), g is the gravitational constant, y is the distance from the supports at the ends of the spanning filament, L is the filament length, E is Young's modulus of the ink ($E \approx 3G$ for the assumption of perfect plasticity) and D is the diameter of the ink. For a deflection of 0.05D at the centre of the cylindrical filament, the minimum storage modulus value (nearly equal to G) can be estimated as following (Eq. (8))

$$G' \geq \frac{1.4(\rho_{ink} - \rho_{med})gL^4}{D^3} \qquad \text{Eq. 8}$$

The minimum storage modulus was reported by Ahn et al., as 2000 Pa [136]. In another study, Rao et al. demonstrated that hexagonal and square-based filaments with similar dimensions require the deposited ink to be stiffer [138]. The maximum deflection for a particular ink deposited through a circular die can also be calculated from its physical properties (see Eq. (9)) [115].

$$\Delta_{max} = \frac{10(\rho_{ink} - \rho_{med})gD^2}{47E} \qquad \text{Eq. 9}$$

In this regard, M'Barki proposed that the yield stress of ink should be high enough to oppose the gravitational force and capillary forces [141]. It is experimentally validated that the shape fidelity of the printed filaments of boehmite inks exceeds 90 % and the sintered density reaches 97 % in that case.

5.3.3.4. Shape retention. Inks with hard-to-control flow behaviour necessitate close control of the extrusion velocity concerning ink rheology to prevent liquid phase migration. Accordingly, material deposition speed varies and so should the speed of the moving stage. This is not practical due to the possible deformation of the extruded filaments by inertial effects. Instead, inks with predictable viscosities are commonly extruded at constant velocities according to a predetermined optimum printing speed for construct uniformity. Hence *a priori* rheological characterisation and optimization are required to perform smooth deposition. The magnitude of ink viscosity is critical for the shape evolution of the filament as it leaves the nozzle. Ideally, the filament should keep the shape of the contours in the nozzle die, but it can return to a shape with lower surface energy if it has low viscosity and enough time. The characteristic time that permits a non-setting ink to restore its unreformed shape is given by Rao et al. (Eq. (10)) [138]:

$$t = \frac{l\eta}{\gamma} \qquad \text{Eq. 10}$$

where l is approximately the length of the nozzle, η is the shear viscosity and γ is the surface tension of the ink [138]. For a typical aqueous ceramic suspension of viscosity around 100 Pa s and surface tension around 50 mN/m, passing through a nozzle of 1 mm length, the filament can flow back to its undeformed shape if the deposition happens slower than 0.5 mm/s (edges become curves and surface features like corners disappear). This is especially important if the ink does not undergo a rapid shift from viscous to the elastic character during the deposition for example by quick drying. So it is generally advised to engineer the ink for induction of a phase change and to keep the deposition rate above a certain limit.

5.3.3.5. Nozzle clogging. Clogging is known as one of the other challenges in DW, which occurs mostly in DW of bone cement injection due to insufficient manual pressurising, while motor-driven high pressures were seen to adequately inject most suspensions [109] [165]. Manual pressurising results in the immobility of the solid particles while the liquid binder can percolate around them, facilitating mat formation and degradation of the ink prior to eventual clogging. A deforming region around a plug core (see Fig. 10) is the desired velocity profile for stable flow and prevention of phase migration. Such partial plug flow at the core also promotes filament shape retention upon deposition [101].

Additive manufacturing of cementitious composites that has been successfully practiced for over a decade by the civil engineering industry is the closest technology to the filament deposition of cementitious inks. Macro-structures are effectively made of construction cement using hose-like nozzles without clogging due to their considerably long setting times and stable flow behaviour [166]. In this case, hydrating particles have a relatively small size in comparison to the large nozzle diameter.

Hence flow stability of inks can be improved by determination of the contiguous slip-enabling critical shear stress, correlating this property to the true shear rate at the wall (proportional to the volumetric flow rate), and adjusting the correlation coefficient (ink viscosity) by chemical or physical means to enable partial plug flow of the ink. Smay et al. successfully demonstrated this approach by varying the pH of non-setting lead zirconate titanate inks, viscoelastic properties of the suspension pH's strong functions [167]. For more complex inks involving time dependency like cements, more rigorous monitoring and control of the wall slip parameters is essential. Generally, the ink is aimed to possess a low critical slip velocity resulting in low critical shear stresses, which reduces the risk of flow instabilities. Determination of the critical slip velocity is possible empirically by analysing the slip behaviour, i.e. the relation between applied stresses and slip velocities in capillary and rotational rheometers [106].

5.3.4. DIW of ceramic composites

DIW printable mix is what can be considered as hardened cementitious composite and is comprised of three main ingredients: a binder or precursor, aggregate, and an activator. The binder is classified as the main ingredient which holding other components of the mixture together and is required for any mix to gain strength. Currently, the most widely available binder in cementitious composites is Ordinary Portland Cement (OPC), and several studies [168,169] have shown its usefulness when incorporated in DIW as it can generate adequate mechanical performance. Tri-calcium silicates (C3S) and di-calcium silicate (C2S) are known as the principal silicate compounds of OPC. Although these particles are stoichiometrically similar to each other, they generate a different amount of hydration products called Portlandite (CH), calcium silica hydrate (C–S–H), and Entringite (AFt). Besides the widespread utilisation of OPC and its high strength gain, several alternative binders, including mineral-based waste materials (e.g. chamotte and alumina-zirconia-silica) [170], nano-clays (e.g. Kaolinite clay and Metakaoline) [171], ashes (e.g. fly ash) [172], and slags (e.g. Ground Granulated Blast-furnace Slag) [173], have recently been widely employed due to their more environmentally friendly nature. This is because the production of OPC involves high CO_2 emissions along with a high energy demand leading to global concern about the use of OPC and greater pressure on industries to look into alternatives to OPC that are more environmentally friendly. The aforementioned binder materials are widely used due to their amorphous or poor crystalline microstructure as well as their aluminosilicate-rich nature. These materials are highly reactive and can generate a hardened structure (C-A-S-H) with high mechanical strength, durability, and enhanced physical properties when subjected to an alkaline reaction [170]. The existence of alkaline solutions such as sodium silicate, sodium carbonate, sodium hydroxide, potassium silicate, potassium hydroxide, Tetra-methyl-ammonium hydroxide [174] and, hybrid of these activators in the mix formulation of Alkali Activated Materials (AAM) and their concentration are reported to have a remarkable impact on the fresh and hardened properties of AAMs. Therefore, the selection of the correct alkaline solution in terms of type and ratio (i.e. ratio between the precursor and the liquid component) is pivotal to ease of the dissolution phase, as it plays the role of the medium through which dissolved aluminosilicates ions can move [175]. The AAM's exact reaction mechanism has not been entirely understood. However, several articles indicate that it relates to the precursor and the alkaline solution's type and ratio. The utilisation of different binders and alkaline activator solutions generates several changes in the AAMs reaction chemistry, altering the hardened objects' final characteristics and quality. Hence, several scholars have tried to identify and explain the different phases of alkali-activation. For instance, Khale et al. indicated that the alkali-activation reaction involved mechanism occurs in two steps: (i) releasing of alumina, silica, and lime; followed by (ii) generation of hydrated calcium aluminosilicate (C-A-S-H) [176]. In other words, as proposed by Duxson et al. the powder aluminosilicate source is first dissolved via alkaline hydrolysis, consuming water and releasing aluminates and silicates monomers. The aforementioned monomers then combine, leading to form dimers, trimers, etc. By increasing the mixture's pH, the dissolution process is accelerated. Hence the solution concentration increases, creating a gel structure. The system continues rearranging and generating new gel networks until a three-dimensional structure is established, which determines the principal components of the AAMs [177].

The major advancement in DIW over the past years involves the incorporation of reinforcing additives. Due to the brittle nature, poor tensile and flexural strength, as well as possessing low strain capacity of cementitious composite structures, different categories of additives, including fibers [178] and nanoparticles [179] are considered as reinforcing agents [180]. These reinforcing additives have the ability to adjust the workability of fresh mixtures and also control the crack propagation in the hardened state [181]. One of the main advantages of the DW and 3D printing over conventional manufacturing processes is the ability to manufacture complex functional structures. Printed parts have a high ratio of porosity comparing to conventional manufacturing processes. While for bone and tissue in-situ applications high porosity ratio could be considered as one of the main advantages of robocasting. However, due to the high ratio of porosity and poor interlayer bonding, printed parts often suffer from the lack of sufficient mechanical strength. To improve mechanical properties several studies have been conducted to determine the influence of reinforcement additives. Zhao et al. studied the influence of polylactic-co-glycolic acid (PLGA) Fiber on 3D printing of the CaP Scaffolds for Osteoanagenesis [182]. Their observations showed that the ultimate tensile strength of CaP with 3 % PLGA is two times more than the corresponding mix without PLGA [182]. The additives are added to the paste to enhance different physical properties. Adding Sodium alginate to CaP paste improves the antibacterial release of the paste while makes the young modulus as low as 1.3 MPa [98]. Cella et al. proposed that adding Poly(caprolactone) (PCL) to CaP increases the scaffold flexural strength, modulus, and fracture toughness [183]. Xiong et al. studied the effects of SiC particles, sintering temperature on the microstructure, composition, and related properties of

PCS-based slurries with various SiCp addition [184]. It is shown that during sintering at 1200 °C, increasing the ratio of SiCp/PCS decreases the weight loss and linear shrinkage and increases the tensile strength and density [184].

Jiang et al. studies the influence of gellan gum (GG) and thermal treatment of 3D printed Poly(tetrafluoroethylene) (PTFE) [185]. Their studies revealed that the additives incorporation could also improve the hydrophobicity, chemical resistivity, and biocompatibility of the PTFE while mechanical properties remain similar to 3D printed PTFE without additives [185]. Mondal et al. studied the influence of nozzle diameter on mechanical properties of robocasting manufactured part by polyethylene glycol diacrylate (PEGDA)/nanohydroxyapatite (nHA)-based nanocomposites [186]. Their observations show that reducing nozzle diameter highly increases the ultimate tensile strength, tensile modulus, and toughness. The toughness of printed parts is significantly higher than the casted part. Furthermore, the Ultimate strength of the printed part by 0.21 mm nozzle is more than twice of the casted part with the same material [186]. Coppola et al. studied 3D printing of Alkali-activated pastes (AAM) with Poly(methyl methacrylate) (PMMA) as an additive [139]. Their observation shows that the bending strength of the sample is approximately 45 MPa, which is higher than the bending strengths of casted material.

Although strength is important in DIW, the rheological properties of the paste are equally as significant. High-viscosity mixtures require high printing pressure to flow material through the nozzle. This could lead to nozzle clogging, inconsistency in material deposition, and entrapment of the material in the extruder. On the contrary, low viscosity causes material flow under the weight of the ink, nozzle leakage, and lack of shape retention after deposition. Consequently, it is necessary to modify the rheological properties in order to print accordingly. Therefore, the inclusion of additives such as poly(acrylic acid) sodium salt [170], poly (ethylenglycole) PEG [187], nano-MgO [188], silica fume [178], Polyvinylpyrrolidone (PVP, 1-ethenyl-2-pyrrolidinone homopolymer) [189], α-TCP PHA(Polyhydroxyalkanoate) Nanoparticles, Na2HPO4 (Disodium phosphate) [125], Hydroxypropyl methylcellulose (HPMC) [190], Poly (ethyleneimine) (PEI) [190], can affect the rheology of mixtures by inducing the thixotropy behaviour and facilitated the printing performance of mixtures at high dimensional resolutions. Sajadi et al. reported that the inclusion of rheology-modifier additives into a mix subsequently could have a large impact on the fresh properties, i.e. increasing the yield shear stress and storage modulus of the fresh mixtures improving shape retention of mixtures after deposition, making it suitable for DIW [169]. For instance, In recent years, new emerging functional nanomaterials such as graphene-based materials (GBMs), including graphene nanoplatelets (GNP), nano graphite (nG) [191], and graphene oxide (GO) [192] have become widely used as rheology modifier agents for cementitious materials as they are able to impart a shear-thinning/thixotropy and an adequate viscosity behaviour within the fresh mixture [193]. It should be noticed that the inclusion of nanoparticles can potentially impede the mechanical enhancement of cementitious composites due to the agglomeration of nanoparticles serving as defects within the hardened structure. This means that the additives in the form of nanoparticles should be dispersed through the matrices. Therefore, dispersion methods such as ultrasonication and high shear mixing as well as dispersing agent materials such as Dispersant high molecular urea modified medium polar polyamide (BYK 430) [178], Ammonium polyacrylate (PAANH4) [189], Dispersant Darvan® 821 A (Sodium Polymethacrylate) [190] have been commonly employed in order to overcome this phenomenon. The dispersant or dispersing agents refer to the substances incorporated into the suspension in order to improve the separation of the particles, prevent agglomeration of the suspensions, and prevent the ink's fast setting. The use of robocasting, especially cementitious composites, makes it the most used process for printing in-situ bone and tissue prosthesis [101,110,119,120,123–126,194]. It is mainly due to the ability of stem cell delivery, growth factor and drug delivery, and revascularization of CPC scaffolds [195]. The robocasting also widely used in: functionally ceramic graded material [196], transparent ceramics and optic [129,130], electronics and insulation [131–135,141], porous media and membrane [139].

6. Discussion

DW brings opportunities for manufacturing complex parts with new multi-functional materials. DW enables design freedom, rapid manufacturing, and limited material waste. This technology has shown great application window from prototyping to high-end production.

Further advances on DW require ink and printer development. This must be with regard to the part performance, desire printing scale and, printer structure of the final product. Part performances include sufficient mechanical properties, working environment, roughness, adhesion of the layers, and resolution of the deposited beads. Several challenges with DW processes which must be contemplated include the complexities in the interaction between hardware, software and the material behaviour used for printing, currently there is limited understanding on these interconnected processes. With a comprehensive understanding on the aforementioned categories and their individual constituent parameters, accurate modelling of the process and eventually optimization of the process parameters according to the desire performance will be possible. As an example, additives including reinforcement agent, rheology modifiers and plasticisers, all need to be understood in terms of their role in modifying mechanical property of the printed final object. The mixture composition must ensure the fluidability and shape retention of deposited beads while possessing sufficient performance once manufactured. In addition to material mixture design, extruder mechanism and hopper set-up, influence the material deposition quality and therefore final product performance. The role of extruder becomes more prominent in the case of thixotropic materials, where the viscosity is time-dependent. In this case applying shear stress on the material in the extruder contributes to delays in ink setting. Therefore, mixture design and its theological properties must be suitable for the extruder being used. The extruder design is especially more important in the case of robocasting where there is no external source of energy influencing shape retention and solidification of the deposited paste. The extruder structure must ensure paste flows in the extruder through the nozzle.

7. Conclusions

An inclusive review of DW printing processes, materials, applications, and current state of the art in various industries was carried out. The main challenges attributed to the development of new materials were also discussed.

The extrusion-based AM processes or DW (called Robocasting for ceramics) are the emerging technologies enabling manufacture of complex, functional, and high-end precision macron-scale parts. DW is divided into three main categories: extrusion-based, energy-assisted and droplet-based technologies. Among all the DW processes, robocasting is the most common and cost-efficient. DW enables manufacturing of different kinds of materials such as metals, biomaterials, polymers, ceramics, slurry pastes, colloidal, and drugs. This enables the manufacturing of a wide range of dimensions scaling from sub-micron to several millimetres for different applications such as biomedical, packaging, electronics and electrics, and in-situ prosthesis. DW could also be used to manufacture multi-material, multi-colour, and shape memory parts.

Printed parts manufactured by DW usually suffer from a lack of sufficient mechanical properties. This is mainly because the parts are manufactured layer by layer which leads to a high ratio of porosity and lack of cohesion between the deposited beads. Therefore, process parameters and ink additives must be selected appropriately through in-depth optimization and long loop of trial and error, this makes it more challenging and less feasible at first, but once the optimum conditions

and parameter are found, it presents great opportunities for niche developments. For the ink additives, the curing agents (for energy-assisted DW), the volatile solvent (for SC-DW), rheology modifier, mechanical strength enhancement agents, and drug delivery can be mentioned.

This review shows the huge number of studies that have been focusing on development of new materials to broaden the applications of DW, where it could be concluded that the optimization of the rheological properties such as injectability and setting time or improvements in the ink composition, ink property, and extruder design are the critical points for achievement of this goal.

Credit author statement

Shahriar Bakrani Balani, Seyed Hamidreza Ghaffar, Mehdi Chougan, Eujin Pei, Erdem Şahin. **Shahriar Bakrani Balani: Data curation, Methodology, Writing - review & editing,** Seyed Hamidreza Ghaffar: Conceptualization, Methodology, Supervision, Writing - review & editing. Mehdi Chougan: Writing - original draft, Data curation. Eujin Pei: Writing - review & editing. Erdem Şahin: Writing - review & editing.

Declaration of competing interest

None.

Acknowledgments

This work was funded as part of the DiWoCiS project, which has received funding from the Newton Fund Institutional Links Grants - British Council.

References

[1] T.D. Ngo, A. Kashani, G. Imbalzano, K.T.Q. Nguyen, D. Hui, Additive manufacturing (3D printing): a review of materials , methods , applications and challenges, Compos. Part B. 143 (2018) 172–196, https://doi.org/10.1016/j.compositesb.2018.02.012.

[2] J.A. Lewis, G.M. Gratson, Direct writing in three dimensions, Mater. Today (2004) 32–39.

[3] J. Cesarano, A review of robocasting technology, Mater. Res. Soc. Symp. Proc. (2021) 133–139.

[4] T. Han, A. Nag, N. Afsarimanesh, S.C. Mukhopadhyay, Laser-assisted printed flexible Sensors : a review, Sensors (2019) 1–28, https://doi.org/10.3390/s19061462.

[5] N.J. Wilkinson, M.A.A. Smith, R.W. Kay, R.A. Harris, A review of aerosol jet printing — a non-traditional hybrid process for micro-manufacturing, Int. J. Adv. Manuf. Technol. (2019) 4599–4619.

[6] X. Zhang, X. Jia, X. Wang, Direct Ink Writing of Polymers and Their Composites, and Related Applications, Elsevier Inc., 2020, https://doi.org/10.1016/B978-0-12-819535-2/00013-2.

[7] J.A. Lewis, J.E. Smay, J. Stuecker, J. Cesarano, Direct ink writing of three-dimensional ceramic structures, J. Am. Ceram. Soc. 89 (2006) 3599–3609, https://doi.org/10.1111/j.1551-2916.2006.01382.x.

[8] C. Chen, X. Wang, Y. Wang, D. Yang, F. Yao, W. Zhang, B. Wang, G.A. Sewvandi, D. Yang, D. Hu, Additive manufacturing of piezoelectric materials, Adv. Funct. Mater. (2020), https://doi.org/10.1002/adfm.202005141.

[9] R. Daly, T.S. Harrington, G.D. Martin, I.M. Hutchings, Inkjet printing for pharmaceutics – a review of research and manufacturing, Int. J. Pharm. 494 (2015) 554–567, https://doi.org/10.1016/j.ijpharm.2015.03.017.

[10] G.D. Martin, S. Hoath, I. Hutchings, Inkjet printing - the physics of manipulating liquid jets and drops, J. Phys. (2008), https://doi.org/10.1088/1742-6596/105/1/012001.

[11] H. Shahariar, I. Kim, H. Soewardiman, J.S. Jur, Inkjet printing of reactive silver ink on textiles, ACS Appl. Mater. Interfaces 11 (2019) 6208–6216, https://doi.org/10.1021/acsami.8b18231.

[12] A. Al-Halhouli, L. Al-Ghussain, S. El Bouri, H. Liu, D. Zheng, Fabrication and evaluation of a novel non-invasive stretchable and wearable respiratory rate sensor based on silver nanoparticles using inkjet, Polymers 11 (2019), https://doi.org/10.3390/polym11091518.

[13] H.K. Cader, G.A. Rance, M.R. Alexander, A.D. Gonçalves, C.J. Roberts, C.J. Tuck, R.D. Wildman, Water-based 3D inkjet printing of an oral pharmaceutical dosage form, Int. J. Pharm. 564 (2019) 359–368, https://doi.org/10.1016/j.ijpharm.2019.04.026.

[14] M. Rosa, P.N. Gooden, S. Butterworth, P. Zielke, R. Kiebach, Y. Xu, C. Gadea, V. Esposito, Zirconia nano-colloids transfer from continuous hydrothermal synthesis to inkjet printing, J. Eur. Ceram. Soc. 39 (2019), https://doi.org/10.1016/j.jeurceramsoc.2017.11.035.

[15] O. Kiefer, J. Breitkreutz, Comparative investigations on key factors and print head designs for pharmaceutical inkjet printing, Int. J. Pharm. 586 (2020) 119561, https://doi.org/10.1016/j.ijpharm.2020.119561.

[16] K. Zhu, D. Yang, Z. Yu, Y. Ma, S. Zhang, R. Liu, J. Li, J. Cui, H. Yuan, Additive manufacturing of Si 2 – Al2O3 refractory products via direct ink writing, Ceram. Int. 46 (2020) 27254–27261, https://doi.org/10.1016/j.ceramint.2020.07.210.

[17] L. Nayak, S. Mohanty, S.K. Nayak, A review on inkjet printing of nanoparticle inks for, J. Mater. Chem. C. (2019) 8771–8795, https://doi.org/10.1039/c9tc01630a.

[18] L. Iftimi, M. Edinger, D. Bar-shalom, J. Rantanen, N. Genina, European Journal of Pharmaceutics and Biopharmaceutics Edible solid foams as porous substrates for inkjet-printable pharmaceuticals, Eur. J. Pharm. Biopharm. 136 (2019) 38–47, https://doi.org/10.1016/j.ejpb.2019.01.004.

[19] K. Liao, C. An, C. Lo, Mechatronics Continuous inkjet-patterned and flashlight-sintered strain sensor for in-line off-axis detection in Roll-to-Roll manufacturing, Mechatronics 59 (2019) 95–103, https://doi.org/10.1016/j.mechatronics.2019.03.006.

[20] D. Zhu, Z. Wang, D. Zhu, Highly conductive graphene electronics by inkjet printing, J. Electron. Mater. (2020), https://doi.org/10.1007/s11664-019-07920-1.

[21] A. Sajedi-moghaddam, E. Rahmanian, N. Naseri, Inkjet printing technology for supercapacitor Application : current state and perspectives, Appl. Mater. Interfaces (2020), https://doi.org/10.1021/acsami.0c07689.

[22] S.F. Pond, X. Corporation, N. York, Drop-on-demand ink jet transducer effectiveness. Recent Prog. Inkjet Technol., 1994, pp. 2–5.

[23] F. Zhang, Y. Ma, Y. Kondo, V. Breedveld, R.P. Lively, A guide to solution-based additive manufacturing of polymeric structures : ink design , porosity manipulation , and printing strategy, Adv. Manuf. Process. (2019) 1–17, https://doi.org/10.1002/amp2.10026.

[24] C.G. Roessler, R. Agarwal, M. Allaire, E.T. Yukl, D. Zhu, M. Bommer, A. S. Brewster, M.C. Browne, R. Chatterjee, E. Cho, A.E. Cohen, Acoustic injectors for drop-on-demand serial femtosecond crystallography, Structure (2016) 1–10, https://doi.org/10.1016/j.str.2016.02.007.

[25] S. Kamisukil, S.E. Corporation, S. Epson, A low power, small, electrostatically-driven commercial inkjet head, IEEE (1998) 63–68.

[26] X.I.E. Dan, Z. Honghai, S.H.U. Xiayun, X. Junfeng, C.A.O. Shu, Multi-materials drop-on-demand inkjet technology based on pneumatic diaphragm actuator, Sci. China Techynological Sci. 53 (2010) 1605–1611, https://doi.org/10.1007/s11431-010-3149-7.

[27] H. Fayazfar, F. Lirvani, U. Ali, E. Toyserkani, Additive manufacturing of high loading concentration zirconia using high-speed drop-on-demand material jetting, Int. J. Adv. Manuf. Technol. (2020), https://doi.org/10.1007/s00170-020-05829-2.

[28] E. Davoodi, H. Fayazfar, F. Liravi, E. Jabari, E. Toyserkani, Drop-on-demand high-speed 3D printing of fl exible milled carbon fi ber/silicone composite sensors for wearable biomonitoring devices, Addit. Manuf. 32 (2020) 101016, https://doi.org/10.1016/j.addma.2019.101016.

[29] B. Nan, F.J. Galindo-Rosales, J.M.F. Ferreira, 3D printing vertically: direct ink writing free-standing pillar arrays, Mater. Today 35 (2020) 16–24, https://doi.org/10.1016/j.mattod.2020.01.003.

[30] A. Ehsan, N. Asli, J. Guo, P.L. Lai, R. Montazami, High-yield production of aqueous graphene for electrohydrodynamic drop-on-demand printing of biocompatible conductive patterns, Biosensors (2020), https://doi.org/10.3390/bios10010006.

[31] H.E. Orimi, S. Sara, H. Kolkooh, E. Hooker, Drop-on-demand cell bioprinting via laser induced side transfer (LIST), Sci. Rep. (2020) 1–9, https://doi.org/10.1038/s41598-020-66565-x.

[32] H. Lee, S.M. Jung, S. Yoon, W.H. Yoon, T.H. Park, S. Kim, H.W. Shin, D.S. Hwang, S. Jung, Immobilization of planktonic algal spores by inkjet printing, Sci. Rep. (2019) 1–7, https://doi.org/10.1038/s41598-019-48776-z.

[33] E. Masaeli, C. Marquette, Direct-write bioprinting approach to construct multilayer cellular tissues, Front. Bioeng. Biotechnol. 7 (2020) 1–8, https://doi.org/10.3389/fbioe.2019.00478.

[34] A. Hamad, A. Mian, S.I. Khondaker, Direct-write inkjet printing of nanosilver ink (UTDAg) on PEEK substrate, J. Manuf. Process. 55 (2020) 326–334, https://doi.org/10.1016/j.jmapro.2020.04.046.

[35] H. Li, Y. Duan, Z. Shao, W. Zhang, H. Li, Morphology-programmable self-aligned microlens array for light extraction via electrohydrodynamic printing, Org. Electron. 87 (2020) 105969, https://doi.org/10.1016/j.orgel.2020.105969.

[36] Z. Zhu, J. Zhang, D. Guo, H. Ning, Z. Zhu, J. Zhang, D. Guo, H. Ning, Functional metal oxide ink systems for drop-on-demand printed thin-film transistors, Langmuir 36 (2020), https://doi.org/10.1021/acs.langmuir.0c00835.

[37] S.I. Moqadam, L. Mädler, A high temperature drop-on-demand droplet generator for metallic melts, Micromachines 477 (2019), https://doi.org/10.3390/mi10070477.

[38] E.B. Secor, Principles of aerosol jet printing, Flex. Print. Electron. (2018), https://doi.org/10.1088/2058-8585/aace28 Manuscript.

[39] P. Dybdahl, P. Bach, A.D. Jensen, Two-fluid spray atomisation and pneumatic nozzles for fluid bed coating/agglomeration purposes : a review, Chem. Eng. Sci. 63 (2008) 3821–3842, https://doi.org/10.1016/j.ces.2008.04.014.

[40] D. Zhao, T. Liu, M. Zhang, R. Liang, B. Wang, Fabrication and characterization of aerosol-jet printed strain sensors for multifunctional composite structures, Smart Mater. Struct. 115008 (2012), https://doi.org/10.1088/0964-1726/21/11/115008.

[41] L. Wells, K. Al, M. Smith, Q. Jing, U.F. Keyser, N. Cati, J. Cama, S. Kar-narayan, Aerosol-jet printing facilitates the rapid prototyping of microfluidic devices with

versatile geometries and precise channel functionalization ′ c, Appl. Mater. Today. 19 (2020), https://doi.org/10.1016/j.apmt.2020.100618.
[42] E.S. Rosker, M.T. Barako, E. Nguyen, D. Dimarzio, K. Kisslinger, D. Duan, R. Sandhu, M.S. Goorsky, J. Tice, Approaching the practical conductivity limits of aerosol jet printed silver, ACS Appl. Mater. Interfaces (2020), https://doi.org/10.1021/acsami.0c06959.
[43] K. Parate, S. V Rangnekar, D. Jing, D.L. Mendivelso-perez, S. Ding, E.B. Secor, E. A. Smith, J.M. Hostetter, M.C. Hersam, J.C. Claussen, Aerosol-jet-printed graphene immunosensor for label-free cytokine monitoring in serum, ACS Appl. Mater. Interfaces (2020), https://doi.org/10.1021/acsami.9b22183.
[44] N.J. Wilkinson, R.W. Kay, R.A. Harris, Electrohydrodynamic and aerosol jet printing for the copatterning of Polydimethylsiloxane and graphene platelet inks, Adv. Mater. Technol. (2020), 2000148, https://doi.org/10.1002/admt.202000148.
[45] A. Hohnholz, K. Obata, Y. Nakajima, J. Koch, M. Terakawa, O. Suttmann, Hybrid UV Laser Direct Writing of UV-Curable PDMS Thin Film Using Aerosol Jet Printing, 2019, https://doi.org/10.1007/s00339-018-1902-0.
[46] G.L. Goh, S. Agarwala, W.Y. Yeong, Aerosol-jet-printed preferentially aligned carbon nanotube twin- lines for printed electronics, ACS Appl. Mater. Interfaces (2019), https://doi.org/10.1021/acsami.9b15060.
[47] L.J. Deiner, T. Jenkins, T. Howell, M. Rottmayer, Aerosol jet printed polymer composite electrolytes for solid-state Li-ion batteries, Adv. Eng. Mater. (2019), https://doi.org/10.1002/adem.201900952.
[48] A. Selimis, V. Mironov, M. Farsari, Microelectronic Engineering Direct laser writing : principles and materials for scaffold 3D printing, Microelectron. Eng. 132 (2015) 83–89, https://doi.org/10.1016/j.mee.2014.10.001.
[49] S. Maruo, O. Nakamura, S. Kawata, Three-dimensional microfabrication with two-photon-absorbed photopolymerization, Opt. Lett. 22 (1997) 132–134.
[50] G. Witzgall, R. Vrijen, E. Yablonovitch, V. Doan, B.J. Schwartz, Single-shot two-photon exposure of commercial photoresist for the production of three-dimensional structures, Opt. Lett. 23 (1998) 1745–1747.
[51] B.Y. Jun, P. Nagpal, D.J. Norris, Thermally stable organic – inorganic hybrid photoresists for fabrication of photonic band gap structures with direct laser writing, Adv. Mater. 20 (2008) 606–610, https://doi.org/10.1002/adma.200702021.
[52] M. Malinauskas, P. Danilevicius, D. Baltriukiene, M. Rutkauskas, A. Zukauskas, Z. Kairyte, G. Bickauskaite, V. Purlys, D. Paipulas, V. Bukelskiene, R. Gadonas, 3D Artificial polymeric scaffolds for stem cell growth fabricated by femtosecond laser, Lithouanian J. Phys. 50 (2010) 75–82, https://doi.org/10.3952/lithjphys.50121.
[53] P. Su, Q.A. Tran, J.J. Fong, K.W. Eliceiri, B.M. Ogle, P.J. Campagnola, Mesenchymal stem cell interactions with 3D ECM modules fabricated via multiphoton excited photochemistry, Biomaromolecules (2012) 2917–2925, https://doi.org/10.1021/bm300949k.
[54] F. Claeyssens, E.A. Hasan, A. Gaidukeviciute, D.S. Achilleos, A. Ranella, C. Reinhardt, A. Ovsianikov, X. Shizhou, C. Fotakis, M. Vamvakaki, B. N. Chichkov, M. Farsari, Three-dimensional biodegradable structures fabricated by two-photon polymerization, Langmuir 55 (2009) 3219–3223, https://doi.org/10.1021/la803803m.
[55] Z. Li, Z. Hong, Y. Xiao, Q. Hao, R. Liang, Thermal effects in single-point curing process for pulsed infrared laser-assisted 3D printing of optics, 3D Print. Addit. Manuf. 7 (2020), https://doi.org/10.1089/3dp.2020.0023.
[56] T. Komori, T. Furukawa, M. Iijima, S. Maruo, Multi-scale laser direct writing of conductive metal microstructures using a 405-nm blue laser, Opt Express 28 (2020) 8363–8370, https://doi.org/10.1364/OE.388593.
[57] S.K. Parupelli, S. Desai, Hybrid additive manufacturing (3D printing) and characterization of functionally gradient materials via in situ laser curing, Int. J. Adv. Manuf. Technol. (2020) 543–556, https://doi.org/10.1007/s00170-020-05884-9.
[58] M. Del Pozo, C. Delaney, C.W.M. Bastiaansen, D. Diamond, A.P.H.J. Schenning, L. Florea, Direct laser writing of 4D micro-structural color actuators using a photonic-photoresist, ACS Nano (2020), https://doi.org/10.1021/acsnano.0c02481.
[59] P. Peng, L. Li, P. He, Y. Zho, J. Fu, Y. Huang, W. Guo, One-step selective laser patterning of copper/graphene flexible electrodes, Nanotechnology (2019), https://doi.org/10.1088/1361-6528/aafe4c.
[60] M.A. Skylar-scott, S. Gunasekaran, J.A. Lewis, Laser-assisted direct ink writing of planar and 3D metal architectures. Proceeding Natl. Acad. Sci, . United States Am., 2016, pp. 6137–6142, https://doi.org/10.1073/pnas.1525131113.
[61] A.C. Lamont, M.A. Restaino, M.J. Kim, R.D. Sochol, A facile multi-material direct laser writing strategy, Lab Chip 19 (2019), https://doi.org/10.1039/c9lc00398c.
[62] W. Liu, Y. Huang, Y. Peng, M. Walczak, D. Wang, Q. Chen, Z. Liu, L. Li, Stable wearable strain sensors on textiles by direct laser writing of graphene, ACS Appl. Nano Mater. (2020), https://doi.org/10.1021/acsanm.9b01937.
[63] P.J. Scott, D.A. Rau, J. Wen, M. Nguyen, C.R. Kasprzak, C.B. Williams, T.E. Long, Polymer-inorganic hybrid colloids for ultraviolet-assisted direct ink write of polymer nanocomposites, Addit. Manuf. 35 (2020) 101393, https://doi.org/10.1016/j.addma.2020.101393.
[64] T. Wu, P. Jiang, X. Zhang, Y. Guo, Z. Ji, X. Jia, X. Wang, Additively manufacturing high-performance bismaleimide architectures with ultraviolet-assisted direct ink writing, Mater. Des. 180 (2019) 107947, https://doi.org/10.1016/j.matdes.2019.107947.
[65] T. Wu, P. Jiang, Z. Ji, Y. Guo, X. Wang, F. Zhou, W. Liu, 3D printing of high-performance isocyanate ester thermosets, Macromol. Rapid Commun. (2020) 1–8, https://doi.org/10.1002/mame.202000397, 2000397.
[66] S. Wu, Q. Ze, X. Kuang, R. Zhang, H.J. Qi, R. Zhao, Magnetic multimaterial printing for multimodal shape transformation with tunable properties and shiftable mechanical behaviors, ACS Appl. Mater. Interfaces (2020), https://doi.org/10.1021/acsami.0c13863.
[67] T. V Neumann, M.D. Dickey, Liquid metal direct write and 3D Printing : a review, Adv. Mater. Technol. (2020) 1–16, https://doi.org/10.1002/admt.202000070, 2000070.
[68] L. Zhou, J. Fu, Q. Gao, P. Zhao, Y. He, All-printed flexible and stretchable electronics with pressing or freezing activatable liquid-metal – silicone inks, Adv. Eng. Mater. (2019), https://doi.org/10.1002/adfm.201906683.
[69] A. Rahim, F. Centurion, J. Han, R. Abbasi, M. Mayyas, J. Sun, M.J. Christoe, D. Esrafilzadeh, F. Allioux, M.B. Ghasemian, J. Yang, J. Tang, T. Daeneke, S. Mettu, J. Zhang, H. Uddin, R. Jalili, K. Kalantar-zadeh, Polyphenol-induced adhesive liquid metal inks for substrate-independent direct pen writing, Adv. Funct. Mater. (2020), https://doi.org/10.1002/adfm.202007336.
[70] Y.-G. Park, H. Min, H. Kim, A. Zhexembekova, C.Y. Lee, J.-U. Park, Three-dimensional, high-resolution printing of carbon nanotube/liquid metal composites with mechanical and electrical reinforcement, Nano Lett. 19 (2019) 4866–4872, https://doi.org/10.1021/acs.nanolett.9b00150.
[71] Y. Li, S. Feng, S. Cao, J. Zhang, D. Kong, Printable liquid metal microparticle ink for ultrastretchable electronics, ACS Appl. Mater. Interfaces (2020), https://doi.org/10.1021/acsami.0c15084.
[72] J.W. Boley, E.L. White, G.T. Chiu, R.K. Kramer, Direct writing of gallium-indium alloy for stretchable electronics, Adv. Funct. Mater. (2014), https://doi.org/10.1002/adfm.201303220.
[73] A. Cook, D.P. Parekh, C. Ladd, G. Kotwal, L. Panich, M. Durstock, M.D. Dickey, C. E. Tabor, Shear-driven direct-write printing of room-temperature gallium-based liquid metal alloys, Adv. Eng. Mater. (2019) 1–10, https://doi.org/10.1002/adem.201900400, 1900400.
[74] T. Chen, A. Sun, C. Chu, H. Wu, J. Wang, J. Wang, Z. Li, J. Guo, G. Xu, Rheological behavior of titania ink and mechanical properties of titania ceramic structures by 3D direct ink writing using high solid loading titania ceramic ink, J. Alloys Compd. 783 (2019) 321–328, https://doi.org/10.1016/j.jallcom.2018.12.334.
[75] S. Kim, J. Oh, D. Jeong, J. Bae, Direct wiring of eutectic gallium–indium to a metal electrode for soft sensor systems, ACS Appl. Mater. Interfaces 11 (2019) 20557–20565, https://doi.org/10.1021/acsami.9b05363.
[76] B. Liang, J. Wei, L. Fang, Q. Cao, T. Tu, H. Ren, X. Ye, High-resolution rapid prototyping of liquid metal electronics by direct writing on highly prestretched substrates, ACS Omega (2019), https://doi.org/10.1021/acsomega.9b02440.
[77] X. Ju, W. Yang, S. Gao, Q. Li, Direct writing of microfluidic three-dimensional photonic crystal structures for terahertz technology applications, ACS Appl. Mater. Interfaces (2019), https://doi.org/10.1021/acsami.9b10561.
[78] S. Guo, F. Gosselin, N. Guerin, A. Lanouette, M. Heuzey, D. Therriault, Solvent-cast three-dimensional printing of multifunctional microsystems, Nano.Micro. Small. (2013), https://doi.org/10.1002/smll.201300975.
[79] J. Dong, Y. Li, P. Lin, M.A. Leeflang, S. Van Asperen, K. Yu, N. Tümer, B. Norder, A.A. Zadpoor, J. Zhou, Solvent-cast 3D printing of magnesium scaffolds, Acta Biomater. 114 (2020) 497–514, https://doi.org/10.1016/j.actbio.2020.08.002.
[80] A. Omidinia-anarkoli, R. Rimal, Y. Chandorkar, D.B. Gehlen, L. De Laporte, J. C. Rose, K. Rahimi, Solvent-induced nanotopographies of single micro fibers regulate cell mechanotransduction, ACS Appl. Mater. Interfaces (2019), https://doi.org/10.1021/acsami.8b17955.
[81] S. Bodkhe, P. Ermanni, 3D printing of multifunctional materials for sensing and actuation : merging piezoelectricity with shape memory, Eur. Polym. J. 132 (2020) 109738, https://doi.org/10.1016/j.eurpolymj.2020.109738.
[82] J.O. Hardin, C.A. Grabowski, M. Lucas, M.F. Durstock, J.D. Berrigan, All-printed multilayer high voltage capacitors with integrated processing feedback, Addit. Manuf. 27 (2019) 327–333, https://doi.org/10.1016/j.addma.2019.02.011.
[83] H. Wei, X. Cauchy, I.O. Navas, Y. Abderrafai, K. Chizari, U. Sundararaj, Y. Liu, J. Leng, D. Therriault, Direct 3D printing of hybrid nanofiber-based nanocomposites for highly conductive and shape memory applications, ACS Appl. Mater. Interfaces 11 (2019) 24523–24532, https://doi.org/10.1021/acsami.9b04245.
[84] A. Prasopthum, Z. Deng, I.M. Khan, Z. Yin, B. Guo, J. Yang, Three dimensional printed degradable and conductive polymer scaffolds promote chondrogenic differentiation of chondroptogenitor cells, Biomater. Sci. 8 (2020) 4287–4298, https://doi.org/10.1039/d0bm00621a.
[85] K. Liu, L. Zhu, S. Tang, W. Wen, L. Lu, M. Liu, C. Zhou, B. Lou, Fabrication and evaluation of chitin whiskers/poly(L-lactide) composite scaffold by direct trisolvent-ink writing method for bone tissue engineering, Nanoscale (2020), https://doi.org/10.1039/D0NR04204H.
[86] X. Wan, F. Zhang, Y. Liu, J. Leng, CNT-based electro-responsive shape memory functionalized 3D printed nanocomposites for liquid sensors, Carbon N. Y. 155 (2019) 77–87, https://doi.org/10.1016/j.carbon.2019.08.047.
[87] B. Zhang, S. Hun, S. Barker, D. Craig, R.J. Narayan, J. Huang, Direct ink writing of polycaprolactone/polyethylene oxide based 3D constructs, Prog. Nat. Sci. Mater. Int. (2020), https://doi.org/10.1016/j.pnsc.2020.10.001.
[88] P. Camacho, H. Busari, K. Seims, P. Schwarzenberg, H. Dailey, L. Chow, 3D printing with peptide-polymer conjugates for single-step fabrication of spatially functionalized scaffolds, Biomater. Sci. (2019), https://doi.org/10.1039/x0xx00000x.
[89] N.R. Geisendorfer, R.N. Shah, Effect of polymer binder on the synthesis and properties of 3D- printable particle-based liquid materials and resulting structures, ACS Omega 4 (2019), https://doi.org/10.1021/acsomega.9b00090.

[90] M. Singh, A.P. Haring, Y. Tong, E. Cesewski, E. Ball, R. Jasper, E.M. Davis, B. N. Johnson, Additive manufacturing of mechanically isotropic thin films and membranes via microextrusion 3D printing of polymer solutions, ACS Appl. Mater. Interfaces (2019), https://doi.org/10.1021/acsami.8b22164.

[91] T.J. Hinton, Q. Jallerat, R.N. Palchesko, J.H. Park, M.S. Grodzicki, H. Shue, M. H. Ramadan, A.R. Hudson, A.W. Feinberg, Three-dimensional printing of complex biological structures by freeform reversible embedding of suspended hydrogels, Sci. Adv. (2015).

[92] J. Malda, J. Visser, F.P. Melchels, T. Jüngst, W.E. Hennink, W.J.A. Dhert, J. Groll, D.W. Hutmacher, 25th anniversary Article : engineering hydrogels for biofabrication, Adv. Mater. (2013) 5011–5028, https://doi.org/10.1002/adma.201302042.

[93] B.B. Xie, R.L. Parkhill, W.L. Warren, J.E. Smay, Direct writing of three-dimensional polymer scaffolds using colloidal gels, Adv. Funct. Mater. (2006) 1685–1693, https://doi.org/10.1002/adfm.200500666.

[94] A. El Moumen, M. Tarfaoui, K. Lafdi, Modelling of the temperature and residual stress fields during 3D printing of polymer composites, Int. J. Adv. Manuf. Technol. (2019) 1661–1676, https://doi.org/10.1007/s00170-019-03965-y.

[95] J.A. Lewis, Direct ink writing of 3D functional materials, Adv. Funct. Mater. (2006) 2193–2204, https://doi.org/10.1002/adfm.200600434.

[96] E. Feilden, E. García-tu, F. Giuliani, E. Saiz, L. Vandeperre, Robocasting of structural ceramic parts with hydrogel inks, J. Eur. Ceram. Soc. 36 (2016) 2525–2533, https://doi.org/10.1016/j.jeurceramsoc.2016.03.001.

[97] W. Li, A. Armani, M.C. Leu, R.G. Landers, Methods of extrusion-on-demand for high solids loading ceramic paste in freeform extrusion fabrication. Solid Free, Fabr. Symp., 2015.

[98] H. Sun, C. Hu, C. Zhou, L. Wu, J. Sun, X. Zhou, F. Xing, C. Long, Q. Kong, J. Liang, Y. Fan, X. Zhang, 3D printing of calcium phosphate scaffolds with controlled release of antibacterial functions for jaw bone repair, Mater. Des. 189 (2020) 108540, https://doi.org/10.1016/j.matdes.2020.108540.

[99] C. Kelder, A.D. Bakker, J. Klein-Nulend, D. Wismeijer, The 3D printing of calcium phosphate with k-carrageenan under conditions permitting the incorporation of biological components—a method, J. Funct. Biomater. 9 (2018), https://doi.org/10.3390/jfb9040057.

[100] E. García-tuñon, S. Barg, J. Franco, R. Bell, S. Eslava, E.D. Elia, R.C. Maher, F. Guitian, E. Saiz, Printing in three dimensions with graphene, Mater. Views (2015) 1688–1693, https://doi.org/10.1002/adma.201405046.

[101] Q. Fu, E. Saiz, A.P. Tomsia, Direct ink writing of highly porous and strong glass scaffolds for load-bearing bone defects repair and regeneration, Acta Biomater. 7 (2011) 3547–3554, https://doi.org/10.1016/j.actbio.2011.06.030.

[102] Y. Maazouz, E.B. Montufar, J. Guillem-marti, I. Fleps, C. Ohman, C. Presson, M. Ginebra, Robocasting of biomimetic hydroxyapatite scaffolds using self-setting inks, J. Mater. Chem. B (2014), https://doi.org/10.1039/C4TB00438H.

[103] S. Raymond, Y. Maazouz, E.B. Montufar, R.A. Perez, B. González, J. Konka, J. Kaiser, M. Ginebra, Accelerated hardening of nanotextured 3D-plotted self-setting calcium phosphate inks, Acta Biomater. 75 (2018) 451–462, https://doi.org/10.1016/j.actbio.2018.05.042.

[104] S. Eqtesadi, A. Motealleh, P. Miranda, A. Pajares, A. Lemos, J.M.F. Ferreira, Robocasting of 45S5 bioactive glass scaffolds for bone tissue engineering, J. Eur. Ceram. Soc. 34 (2014) 107–118, https://doi.org/10.1016/j.jeurceramsoc.2013.08.003.

[105] D.M. Kalyon, S. Aktas, Factors affecting the rheology and processability of highly filled suspensions, Annu. Rev. Chem. Biomol. Eng. (2014), https://doi.org/10.1146/annurev-chembioeng-060713-040211.

[106] F. Soltani, Slip velocity and slip layer thickness in flow of, J. Appl. Phys. Sci. 9 (1998) 515–522.

[107] D.M. Kalyon, Apparent slip and viscoplasticity of concentrated suspensions Apparent slip and viscoplasticity of concentrated, J. Rheol. 621 (2005) 621–640, https://doi.org/10.1122/1.1879043.

[108] H.S. Tang, D.M. Kalyon, Time-dependent Tube Flow of Compressible Suspensions Subject to Pressure Dependent Wall Slip : Ramifications on Development of Flow Instabilities Published by the the Society of Rheology Time-dependent Tube Flow of Compressible Suspensions Subject to Pressure Dependent Wall Slip : Ramifications on Development of Flow Instabilities, 2014, p. 1069, https://doi.org/10.1122/1.2955508.

[109] A. Fatimi, J. Tassin, J. Bosco, R. Deterre, M. Axelos, P. Weiss, Injection of calcium phosphate pastes : prediction of injection force and comparison with experiments, J. Mater. Sci. (2012) 1593–1603, https://doi.org/10.1007/s10856-012-4640-4.

[110] J. Franco, P. Hunger, M.E. Launey, A.P. Tomsia, E. Saiz, Direct write assembly of calcium phosphate scaffolds using a water-based hydrogel, Acta Biomater. 6 (2010) 218–228, https://doi.org/10.1016/j.actbio.2009.06.031.

[111] B.S. Ghosh, S.T. Parker, X. Wang, D.L. Kaplan, J.A. Lewis, Direct-write assembly of microperiodic silk fibroin scaffolds for tissue engineering applications, Adv. Funct. Mater. (2008) 1883–1889, https://doi.org/10.1002/adfm.200800040.

[112] B.A. Tuttle, J.E. Smay, J.C. Iii, J.A. Voigt, T.W. Scofield, W.R. Olson, J.A. Lewis, Bruce A. Tuttle, ** james E. Smay, * joseph cesarano III, * james A. Voigt, timothy W. Scofield, and walter R. Olson, J. Am. Ceram. Soc. 74 (2001) 872–874.

[113] A.M. Deliormanlı, M.N. Rahaman, Direct-write assembly of silicate and borate bioactive glass scaffolds for bone repair, J. Eur. Ceram. Soc. 32 (2012) 3637–3646, https://doi.org/10.1016/j.jeurceramsoc.2012.05.005.

[114] X. Lu, Y. Lee, S. Yang, Y. Hao, J.R.G. Evans, C.G. Parini, Solvent-based paste extrusion solid freeforming, J. Eur. Ceram. Soc. 30 (2010) 1–10, https://doi.org/10.1016/j.jeurceramsoc.2009.07.019.

[115] J.E. Smay, J.C. Iii, J.A. Lewis, Colloidal inks for directed assembly of 3-D periodic structures, Langmuir 84 (2002) 5429–5437.

[116] J.C. Conrad, S.R. Ferreira, J. Yoshikawa, R.F. Shepherd, B.Y. Ahn, J.A. Lewis, Current opinion in colloid & interface science designing colloidal suspensions for directed materials assembly, Curr. Opin. Colloid Interface Sci. 16 (2011) 71–79, https://doi.org/10.1016/j.cocis.2010.11.002.

[117] D.J. Hoelzle, A.G. Alleyne, A.J.W. Johnson, Micro-robotic deposition guidelines by a design of experiments approach to maximize fabrication reliability for the bone scaffold application, Acta Biomater. 4 (2008) 897–912, https://doi.org/10.1016/j.actbio.2008.02.018.

[118] P. Miranda, E. Saiz, K. Gryn, A.P. Tomsia, Sintering and robocasting of -tricalcium phosphate sca V olds for orthopaedic applications, Acta Biomater. 2 (2006) 457–466, https://doi.org/10.1016/j.actbio.2006.02.004.

[119] H. Elsayed, M. Secco, F. Zorzi, K. Schuhladen, R. Detsch, A.R. Boccaccini, E. Bernardo, Highly porous polymer-derived bioceramics based on a complex hardystonite solid solution, Materials 1–14.

[120] U. Kiran, S. Malferrari, A. Van Haver, F. Verstreken, S. Narayan, D.M. Kalaskar, Optimization of extrusion based ceramic 3D printing process for complex bony designs, Mater. Des. 162 (2019) 263–270, https://doi.org/10.1016/j.matdes.2018.11.054.

[121] L. Sun, S.T. Parker, D. Syoji, X. Wang, J.A. Lewis, D.L. Kaplan, Direct-write assembly of 3D silk/hydroxyapatite scaffolds for bone Co-cultures, Adv. Healthc. Mater. (2012) 729–735, https://doi.org/10.1002/adhm.201200057.

[122] S. Yang, H. Yang, X. Chi, J.R.G. Evans, I. Thompson, R.J. Cook, P. Robinson, Rapid prototyping of ceramic lattices for hard tissue scaffolds, Mater. Des. 29 (2008) 1802–1809, https://doi.org/10.1016/j.matdes.2008.03.024.

[123] A. Stanciuc, C.M. Sprecher, J. Adrien, L.I. Roiban, M. Alini, L. Gremillard, M. Peroglio, Robocast zirconia-toughened alumina scaffolds: processing, structural characterisation and interaction with human primary osteoblasts, J. Eur. Ceram. Soc. (2017), https://doi.org/10.1016/j.jeurceramsoc.2017.08.031.

[124] N. Xu, X. Ye, D. Wei, J. Zhong, Y. Chen, G. Xu, D. He, 3D artificial bones for bone repair prepared by computed tomography-guided fused deposition modeling for bone repair, ACS Appl. Mater. Interfaces (2014).

[125] E.B. Montufar, Y. Maazouz, M.P. Ginebra, Relevance of the setting reaction to the injectability of tricalcium phosphate pastes, Acta Biomater. 9 (2013) 6188–6198, https://doi.org/10.1016/j.actbio.2012.11.028.

[126] I. Denry, L.T. Kuhn, Design and characterization of calcium phosphate ceramic scaffolds for bone tissue engineering, Dent. Mater. 32 (2015) 43–53, https://doi.org/10.1016/j.dental.2015.09.008.

[127] T. Serra, J.A. Planell, M. Navarro, High-resolution PLA-based composite scaffolds via 3-D printing technology, Acta Biomater. 9 (2013) 5521–5530, https://doi.org/10.1016/j.actbio.2012.10.041.

[128] Y. Li, L. Li, B. Li, Direct write printing of three-dimensional ZrO 2 biological scaffolds, Mater. Des. 72 (2015) 16–20, https://doi.org/10.1016/j.matdes.2015.02.018.

[129] Z. Zhao, G. Zhou, Z. Yang, Direct ink writing of continuous SiO 2 fiber reinforced wave-transparent ceramics, J. Adv. Ceram. 9 (n.d.) 403–412.

[130] I.K. Jones, Z.M. Seeley, N.J. Cherepy, E.B. Duoss, S.A. Payne, Direct ink write fabrication of transparent ceramic gain media, Opt. Mater. 75 (2018) 19–25, https://doi.org/10.1016/j.optmat.2017.10.005.

[131] H. Jin, Z. Yang, J. Zhong, D. Cai, H. Li, D. Jia, Mechanical and dielectric properties of 3D printed highly porous ceramics fabricated via stable and durable gel ink, J. Eur. Ceram. Soc. 39 (2019) 4680–4687, https://doi.org/10.1016/j.jeurceramsoc.2019.07.002.

[132] Z. Lu, Y. Xia, K. Miao, S. Li, L. Zhu, H. Nan, J. Cao, Microstructure control of highly oriented short carbon fibres in SiC matrix composites fabricated by direct ink writing, Ceram. Int. 45 (2019) 17262–17267, https://doi.org/10.1016/j.ceramint.2019.05.283.

[133] Q. Sun, Y. Peng, H. Cheng, Y. Mou, Z. Yang, D. Liang, Direct ink writing of 3D cavities for direct plated copper ceramic substrates with kaolin suspensions, Ceram. Int. 45 (2019) 12535–12543, https://doi.org/10.1016/j.ceramint.2019.03.191.

[134] Y.Y. Aw, K.C. Yeoh, M.A. Idris, L.P. Teh, H. Kheirul Amali, S.A. Sazali, Effect of printing parameters on tensile, dynamic mechanical, and thermoelectric properties of FDM 3D printed CABS/ZnO composites, Materials (2018), https://doi.org/10.3390/ma11040466.

[135] T. An, K. Hwang, J. Kim, J. Kim, Extrusion-based 3D direct ink writing of NiZn-ferrite structures with viscoelastic ceramic suspension, Ceram. Int. 46 (2020) 6469–6476, https://doi.org/10.1016/j.ceramint.2019.11.127.

[136] B.Y. Ahn, E.B. Duoss, M.J. Motala, X. Guo, S. Park, Y. Xiong, J. Yoon, R.G. Nuzzo, J.A. Rogers, J.A. Lewis, Omnidirectional printing of flexible, stretchable, and spanning silver microelectrodes, Science 323 (2009) 1590–1594, 80.

[137] A. Renteria, H. Fontes, J.A. Diaz, J.E. Regis, L.A. Chavez, T.B. Tseng, Optimization of 3D printing parameters for BaTiO 3 piezoelectric ceramics through design of experiments, Mater. Res. Express (2019).

[138] R. Rao, K. Krafcik, A. Morales, J.A. Lewis, Microfabricated deposition nozzles for direct-write assembly of three-dimensional periodic structures **, Adv. Mater. 9 (2005) 289–293, https://doi.org/10.1002/adma.200400514, 0.

[139] B. Coppola, C. Tardivat, J. Tulliani, L. Montanaro, P. Palmero, 3D printing of dense and porous alkali-activated refractory wastes via Direct Ink Writing (DIW), J. Eur. Ceram. Soc. (2021), https://doi.org/10.1016/j.jeurceramsoc.2021.01.019.

[140] P. Biswas, S. Mamatha, S. Naskar, Y. Srinivasa, R. Johnson, G. Padmanabham, 3D extrusion printing of magnesium aluminate spinel ceramic parts using thermally induced gelation of methyl cellulose, J. Alloys Compd. 770 (2019) 419–423, https://doi.org/10.1016/j.jallcom.2018.08.152.

[141] A.M. Barki, L. Bocquet, A. Stevenson, Linking rheology and printability for dense and strong ceramics by direct ink writing, Sci. Rep. (2017), https://doi.org/10.1038/s41598-017-06115-0.

[142] M. Habib, G. Baroud, F. Gitzhofer, M. Bohner, Mechanisms underlying the limited injectability of hydraulic calcium phosphate paste, Acta Biomater. 4 (2008) 1465–1471, https://doi.org/10.1016/j.actbio.2008.03.004.
[143] R.O. Neill, H.O. Mccarthy, E.B. Montufar, M. Ginebra, D.I. Wilson, A. Lennon, N. Dunne, Critical review : injectability of calcium phosphate pastes and cements, Acta Biomater. 50 (2017) 1–19, https://doi.org/10.1016/j.actbio.2016.11.019.
[144] M. Bohner, G. Baroud, Injectability of calcium phosphate pastes, Biomaterials 26 (2004) 1553–1563, https://doi.org/10.1016/j.biomaterials.2004.05.010.
[145] A. Zocca, P. Colombo, C.M. Gomes, G. Jens, Additive manufacturing of ceramics: issues, potentialities, and opportunities, J. Am. Ceram. Soc. 2001 (2015), https://doi.org/10.1111/jace.13700.
[146] W. Liu, J. Zhang, P. Weiss, F. Tancret, J. Bouler, The influence of different cellulose ethers on both the handling and mechanical properties of calcium phosphate cements for bone substitution, Acta Biomater. 9 (2013) 5740–5750, https://doi.org/10.1016/j.actbio.2012.11.020.
[147] M. Komath, H.K. Varma, Development of a fully injectable calcium phosphate cement for orthopedic and dental applications, Bull. Meterial Sci. 26 (2003) 415–422.
[148] S. Tadier, L. Galea, B. Charbonnier, G. Baroud, M. Bohner, Phase and size separations occurring during the injection of model pastes composed of b -tricalcium phosphate powder , glass beads and aqueous solutions, Acta Biomater. 10 (2014) 2259–2268, https://doi.org/10.1016/j.actbio.2013.12.018.
[149] C. Yan, Investigation of FEF process liquid phase migration using orthogonal design of experiments, Rapid Prototyp. J. (2018), https://doi.org/10.1108/RPJ-10-2016-0173.
[150] E.F. Burguera, H.H.K. Xu, L. Sun, Injectable calcium phosphate Cement : effects of powder-to-liquid ratio and needle size, J. Biomed. Mater. Res. B Appl. Biomater. (2007) 493–502, https://doi.org/10.1002/jbmb.
[151] G. Baroud, E. Cayer, M. Bohner, Rheological characterization of concentrated aqueous b -tricalcium phosphate suspensions : the effect of liquid-to-powder ratio, milling time, and additives, Acta Biomater. 1 (2005) 357–363, https://doi.org/10.1016/j.actbio.2005.01.003.
[152] X. Chateau, Particle packing and the rheology of concrete. Underst. Rheol. Concr., Woodhead Publishing Limited, 2012, pp. 117–143, https://doi.org/10.1533/9780857095282.2.117.
[153] K. Ishikawa, Effects of spherical tetracalcium phosphate on injectability and basic properties of apatitic cement, Key Eng. Mater. 242 (2003) 369–372. https://doi.org/10.4028/www.scientific.net/KEM.240-242.369.
[154] I. Khairoun, M.G. Boltong, F.C.M. Driessens, J.A. Planell, Some factors controlling the injectability of calcium phosphate bone cements, J. Mater. Sci. Mater. Med. 9 (n.d.) 425–428.
[155] J.L. Lacout, L. Leroux, Z. Hatim, M. Fre, Effects of various adjuvants (lactic acid , glycerol , and chitosan) on the injectability of a calcium phosphate cement, Bone 25 (1999) 31–34.
[156] G. Baroud, C. Matsushita, M. Samara, L. Beckman, T. Steffen, Influence of oscillatory mixing on the injectability of three acrylic and two calcium-phosphate bone cements for vertebroplasty, J. Biomed. Mater. Res. Part B. (2003) 105–111.
[157] M.J. Patel, S. Blackburn, D.I. Wilson, Modelling of paste ram extrusion subject to liquid phase migration and wall friction, Chem. Eng. Sci. 172 (2017) 487–502, https://doi.org/10.1016/j.ces.2017.07.001.
[158] R.L. Walton, M.A. Fanton, R.J.M. Jr, Dispersion and rheology for direct writing lead-based piezoelectric ceramic pastes with anisotropic template particles, J. Am. Ceram. Soc. (2020) 6157–6168, https://doi.org/10.1111/jace.17350.
[159] E. Sahin, D. Kalyon, The rheological behavior of a fast-setting calcium phosphate bone cement and its dependence on deformation conditions, J. Mech. Behav. Med. Mater. (2017) 252–260, https://doi.org/10.1016/j.jmbbm.2017.05.017.
[160] S.S.L. Chan, M.L. Sesso, G. V Franks, Direct ink writing of hierarchical porous alumina-stabilized emulsions : rheology and printability, J. Am. Ceram. Soc. (2020) 5554–5566, https://doi.org/10.1111/jace.17305.
[161] S. Bakrani Balani, F. Chabert, V. Nassiet, A. Cantarel, C. Garnier, Toward improvement of the properties of parts manufactured by FFF (Fused Filament Fabrication) through understanding the influence of temperature and rheological behaviour on the coalescence phenomenon, in: AIP Conf. Proc. 1896, American Institute of Physics, 2017, https://doi.org/10.1063/1.5008034.
[162] L. Li, Q. Lin, M. Tang, A.J.E. Duncan, C. Ke, Advanced polymer designs for direct-ink-write 3D printing, Chem. Eur J. (2019) 1–15, https://doi.org/10.1002/chem.201900975.
[163] S.S.L. Chan, R.M. Pennings, L. Edwards, G. V Franks, 3D printing of clay for decorative architectural applications : E ff ect of solids volume fraction on rheology and printability, Addit. Manuf. 35 (2020) 101335, https://doi.org/10.1016/j.addma.2020.101335.
[164] E. Şahin, D.M. Kalyon, Preshearing is an in situ setting modification method for inorganic bone cements, Med. Devices Sensors (2020) 1–10, https://doi.org/10.1002/mds3.10105.
[165] P. Yaras, D.M. Kalyon, U. Yilmazer, Flow instabilities in capillary flow of concentrated suspensions, Rheol. Acta 59 (1994) 48–59.
[166] F. Bos, R. Wolfs, Z. Ahmed, T. Salet, Additive manufacturing of concrete in construction : potentials and challenges of 3D concrete printing Additive manufacturing of concrete in construction : potentials and challenges of 3D concrete printing, Virtual Phys. Prototyp. 11 (2016) 209–225, https://doi.org/10.1080/17452759.2016.1209867.
[167] J.E. Smay, Direct ink writing of three-dimensional ceramic structures, J. Am. Ceram. Soc. 3609 (2006) 3599–3609, https://doi.org/10.1111/j.1551-2916.2006.01382.x.
[168] L.A. Vergara, H.A. Colorado, Additive manufacturing of Portland cement pastes with additions of kaolin, superplastificant and calcium carbonate, Construct. Build. Mater. 248 (2020) 118669, https://doi.org/10.1016/j.conbuildmat.2020.118669.
[169] S.M. Sajadi, P.J. Boul, C. Thaemlitz, A.K. Meiyazhagan, A.B. Puthirath, C. S. Tiwary, M.M. Rahman, P.M. Ajayan, Direct ink writing of cement structures modified with nanoscale Additive, Adv. Eng. Mater. (2019) 1–10, https://doi.org/10.1002/adem.201801380, 1801380.
[170] B. Coppola, C. Tardivat, J. Tulliani, L. Montanaro, P. Palmero, 3D printing of dense and porous alkali-activated refractory wastes via Direct Ink Writing (DIW), J. Eur. Ceram. Soc. (2021), https://doi.org/10.1016/j.jeurceramsoc.2021.01.019.
[171] C.F. Revelo, H.A. Colorado, 3D printing of kaolinite clay ceramics using the Direct Ink Writing (DIW) technique, Ceram. Int. (2017), https://doi.org/10.1016/j.ceramint.2017.12.219, 0–1.
[172] B. Panda, M.J. Tan, Experimental study on mix proportion and fresh properties of fly ash based geopolymer for 3D concrete printing, Ceram. Int. (2018), https://doi.org/10.1016/j.ceramint.2018.03.031.
[173] A. Albar, M. Chougan, M.J.A. Kheetan, M. Ra, Effective extrusion-based 3D printing system design for cementitious-based materials, Results Eng 6 (2020), https://doi.org/10.1016/j.rineng.2020.100135.
[174] A. Rincón, H. Elsayed, E. Bernardo, Highly porous cordierite ceramics from engineered basic activation of metakaolin/talc aqueous suspensions, J. Eur. Ceram. Soc. (2020) 1–5, https://doi.org/10.1016/j.jeurceramsoc.2020.06.072.
[175] X. Chen, Y. Guo, S. Ding, H.Y. Zhang, F.Y. Xia, J. Wang, M. Zhou, Utilization of red mud in geopolymer-based pervious concrete with function of adsorption of heavy metal ions, J. Clean. Prod. (2018), https://doi.org/10.1016/j.jclepro.2018.09.263.
[176] D. Khale, R. Chaudhary, Mechanism of geopolymerization and factors influencing its development : a review, J. Mterial Sci. (2007) 729–746, https://doi.org/10.1007/s10853-006-0401-4.
[177] P. Duxson, A. Fernandez-Jimenez, J.l. Provis, G.C. Lukey, A. Palomo, J.S.J. Van Deventer, Geopolymer technology : the current state of the art, J. Mater. Sci. (2007) 2917–2933, https://doi.org/10.1007/s10853-006-0637-z.
[178] G. Franchin, L. Wahl, P. Colombo, Direct ink writing of ceramic matrix composite structures, J. Am. Ceram. Soc. (2017), https://doi.org/10.1111/jace.15045.
[179] S. Tarafder, N.M. Davies, A. Bandyopadhyay, S. Bose, 3D printed tricalcium phosphate bone tissue engineering scaffolds: effect of SrO and MgO doping on in vivo osteogenesis in a rat distal femoral defect model, Biomater. Sci. 1 (2013) 1250–1259, https://doi.org/10.1039/c3bm60132c.
[180] M. Chougan, S. Hamidreza, P. Sikora, S. Chung, T. Rucinska, D. Stephan, A. Albar, M. Ra, Investigation of additive incorporation on rheological , microstructural and mechanical properties of 3D printable alkali-activated materials, Mater. Des. 202 (2021), https://doi.org/10.1016/j.matdes.2021.109574.
[181] M. Chougan, S. Hamidreza, M. Jahanzat, A. Albar, The influence of nano-additives in strengthening mechanical performance of 3D printed multi-binder geopolymer composites, Construct. Build. Mater. 250 (2020) 118928, https://doi.org/10.1016/j.conbuildmat.2020.118928.
[182] G. Zhao, R. Cui, Y. Chen, S. Zhou, C. Wang, Z. Hu, X. Zheng, M. Li, S. Qu, 3D printing of well dispersed electrospun PLGA fiber toughened calcium phosphate scaffolds for Osteoanagenesis, J. Bionic Eng. 17 (2020) 652–668, https://doi.org/10.1007/s42235-020-0051-2.
[183] J. Vella, R. Trombetta, M. Hoffman, J. Inzana, H.A. Awad, D. Benoit, 3D printed calcium phosphate and poly(caprolactone) composites with improved mechanical properties and preserved microstructure, J. Biomed. Mater. Res. (2018) 1–30, https://doi.org/10.1002/jbm.a.36270.
[184] H. Xiong, H. Chen, L. Zhao, Y. Huang, K. Zhou, D. Zhang, SiCw/SiCp reinforced 3D-SiC ceramics using direct ink writing of polycarbosilane-based solution : microstructure , composition and mechanical properties, J. Eur. Ceram. Soc. 39 (2019) 2648–2657, https://doi.org/10.1016/j.jeurceramsoc.2019.02.045.
[185] Z. Jiang, O. Erol, D. Chatterjee, W. Xu, N. Hibino, L.H. Romer, S.H. Kang, D. H. Gracias, Direct ink writing of poly(tetrafluoroethylene) (PTFE) with tunable mechanical properties, ACS Appl. Mater. Interfaces (2019), https://doi.org/10.1021/acsami.9b07279.
[186] D. Mondal, T.L. Willett, Mechanical properties of nanocomposite biomaterials improved by extrusion during direct ink writing, J. Mech. Behav. Biomed. Mater. 104 (2020), https://doi.org/10.1016/j.jmbbm.2020.103653.
[187] G. Franchin, P. Scanferla, L. Zeffiro, H. Elsayed, A. Baliello, G. Giacomello, M. Pasetto, P. Colombo, Direct ink writing of geopolymeric inks, J. Eur. Ceram. Soc. (2017) 1–9, https://doi.org/10.1016/j.jeurceramsoc.2017.01.030.
[188] S. Tang, L. Yang, X. Liu, G. Li, W. Jiang, Z. Fan, Direct ink writing additive manufacturing of porous alumina-based ceramic cores modi fi ed with nanosized MgO, J. Eur. Ceram. Soc. 40 (2020) 5758–5766, https://doi.org/10.1016/j.jeurceramsoc.2020.07.058.
[189] L. Rueschhoff, W. Costakis, M. Michie, J. Youngblood, R. Trice, Additive manufacturing of dense ceramic parts via direct ink writing of aqueous alumina suspensions, Int. J. Appl. Ceram. Technol. 10 (2016) 1–10, https://doi.org/10.1111/ijac.12557.
[190] R.C. Richard, R.N. Oliveira, G.D.A. Soares, R.M.S.M. Thiré, Direct-write assembly of 3D scaffolds using colloidal calcium phosphates inks, Rev. Mater. 19 (2014) 61–67, https://doi.org/10.1590/S1517-70762014000100009.
[191] M. Chougan, E. Marotta, F.R. Lamastra, F. Vivio, G. Montesperelli, U. Ianniruberto, S. Hamidreza, M.J. Al-kheetan, A. Bianco, High performance cementitious nanocomposites : the effectiveness of nano-Graphite (nG), Construct. Build. Mater. 259 (2020), 119687, https://doi.org/10.1016/j.conbuildmat.2020.119687.
[192] M. Chougan, E. Marotta, F.R. Lamastra, F. Vivio, G. Montesperelli, U. Ianniruberto, A. Bianco, A systematic study on EN-998-2 premixed mortars

modified with graphene-based materials, Construct. Build. Mater. 227 (2019) 116701, https://doi.org/10.1016/j.conbuildmat.2019.116701.
[193] G. Zhou, C. Li, Z. Zhao, Y. Qi, Z. Yang, 3D printing geopolymer nanocomposites : graphene oxide size effects on a reactive matrix, Carbon N. Y. 164 (2020) 215–223, https://doi.org/10.1016/j.carbon.2020.02.021.
[194] A.A. Nommeots-nomm, P.D. Lee, R. Julian, Direct ink writing of highly bioactive glasses, J. Eur. Ceram. Soc. (2017), https://doi.org/10.1016/j.jeurceramsoc.2017.08.006.
[195] H.H.K. Xu, P. Wang, L. Wang, C. Bao, Q. Chen, M.D. Weir, L.C. Chow, L. Zhao, X. Zhou, M.A. Reynolds, Calcium phosphate cements for bone engineering and their biological properties, Bone Res 5 (2017) 1–19, https://doi.org/10.1038/boneres.2017.56.
[196] W. Li, A. Armani, A. Martin, B. Kroehler, A. Henderson, T. Huang, J. Watts, G. Hilmas, M. Leu, Extrusion-based additive manufacturing of functionally graded ceramics, J. Eur. Ceram. Soc. 41 (2021) 2049–2057, https://doi.org/10.1016/j.jeurceramsoc.2020.10.029.